PTYS 594a

PLANETARY FIELD GEOLOGY PRACTICUM

Field Trip 19-21 February 1993

Table of Contents

1. your helpful host.
2. your xeriphytic hostess.

PTYS 594a,

PLANETARY FIELD GEOLOGY PRACTICUM

Itinerary, Field Trip 19-21 February 1993

H. J. Melosh, 353 Space Sciences, extension 2806

We will depart at 8:00 am *sharp* on Friday, 19 February from University avenue in front of the LPL "loading dock" in four 8-passanger Suburban vans. Try to be at LPL by 7:30 am to get the vans loaded. Please be sure that you have had breakfast beforehand, have ice for the coolers, etc. before we are scheduled to leave: breakfast and ice runs just before departure have caused long delays in the past!

Our approximate itinerary, as worked out in the last class meeting is:

Friday, 19 February:

8:00 am Distribute handouts, Depart LPL, turn right on Cherry to Speedway, then travel East on speedway to I-10, proceed North to I-8.
10:00 am Stop at Sentinel Volcanic field, discuss Gila graben geology --K. Cyr continue on I-8 to Yuma
12:00 noon Stop at Gray's Well on I-8 for Lunch, discussion of Algodones dunes. Then backtrack on I-8, take exit to S34 (Ogilby rd), drive North through Ogilby to junction with Rte. 78. Proceed ca. 5 mi East on Rte. 78.
1:00 pm Stop to discuss geology of Chocolate Mts., then return West on Rte. 78 to Osborne Park in center of Algodones dune field --A. Rivkin.
2:00 pm Stop at Osborne Park, observe dunes --J. Head
Continue West on Rte. 78 to Brawley, then turn North on Rte 111, then West on S30 to Gentry road, stop at Pumice Buttes, Obsidian Butte on shore of Salton Sea.
4:00 pm Stop at Pumice Buttes, discuss Salton Sea Brines and Geothermal area --J. Stansberry
4:30 pm Drive East on Sinclair road, turn North on Rte. 111 toward Niland, turn East at Niland road to Beal road, cross Coachella canal and stop to observe Lake Cahuilla shorelines --W. Bottke.
5:30 pm Return to Niland, proceed North on Rte 111 to Salt Creek stop, try to locate site of trench and discuss Paleoseismology of Southern San Andreas --J. Grier
7:00 pm Locate campsite near Salt Creek, camp for night. Campfire discussion of the history of Salton Sea --E. Howell

Saturday, 20 February:

8:00 am Break Camp, contine North on Rte 111 to Mecca. Turn right on 66th Ave, drive East to Box Canyon Road, proceed into Mecca Hills.
9:00 am Stop at Mecca Hills, observe recent faulting, flood deposits in floor of canyons -- J. Pedicino.
10:00 am Return to Mecca, continue North on Rte. 111 to Indio (optional stop at Shield's for Date Shakes), continue on I-10 toward Palm Springs. Take Indian Ave. exit West from I-10, park near electric substation.

11:00 am Observe ventifacts at Garnet Hill --D. Dawson
12:00 noon Return to I-10, drive East to Route 62, drive up White Water Alluvial fan. Exit at convient location (lunch), discuss geology of transverse ranges --M. Nolan
1:30 pm Continue North on Rte. 62 to Yucca Valley, turn North on Rte. 247 toward Landers. Exit Rte. 247 at Bessemer Mine road, drive to site of earthquake ground breakage.
2:30 pm Stop to climb over hill and observe fault offset, discuss Landers earthquake sequence --E. Karkoscha.
3:30 pm Return to Rte. 247, continue West to Blackhawk landslide. Stop at snout, observe section in quarry, then proceed as close to head of slide as possible. -- W. Grundy, J. Johnson.
5:30 pm Return to Bessemer Mine road
6:30 pm camp

Sunday, 21 February:

8:00 am Break Camp, drive South on Rte. 247 to Yucca Valley, turn left and proceed East on Rte. 62 to Joshua Tree Park in Twentynine Palms.
10:00 am Stop for geology hike in Joshua Tree park --C. Herron, E. Pierazzo.
12:00 noon Proceed South through park on scenic drive.
1:00 pm Stop for lunch in southern part of Joshua Tree Park.
2:00 pm Proceed East on I-10 toward Blythe, Exit at US 95, proceed North 10 miles.
3:00 pm Stop to observe geoglyphs in desert pavement --C. Steffens
4:00 pm Return to US 95, drive South to Blythe, continue East on I-10 to Tucson (it may be best to avoid Phoenix by taking the Buckeye exit, Rte. 85 south to Gila Bend, then I-8 East to Eloy, where we again pick up I-10).
8:00 pm Arrive Tucson, unpack vans, go home.

Additional Information:

Food Groups: J. Melosh (Vickery, Steffens, Herron, Head, Pierazzo, Kring), A. Rivkin (Nolan, Howell, Grier, Bottke, Hillgren?), D. Dawson (Johnson, Pedicino, Stansberry), plus singlets (Grundy, Cyr, Karkoscha).

Primary Drivers: W. Grundy, M. Nolan, J. Stansberry

Distribution:

W. Bottke
K. Cyr
D. Dawson
J. Grier
W. Grundy
J. Head
C. Herron
V. Hillgren
E. Howell
J. Johnson
E. Karkoscha
D. Kring
M. Nolan
J. Pedicino
E. Pierazzo
A. Rivkin
J. Stansberry
C. Steffens
A. Vickery

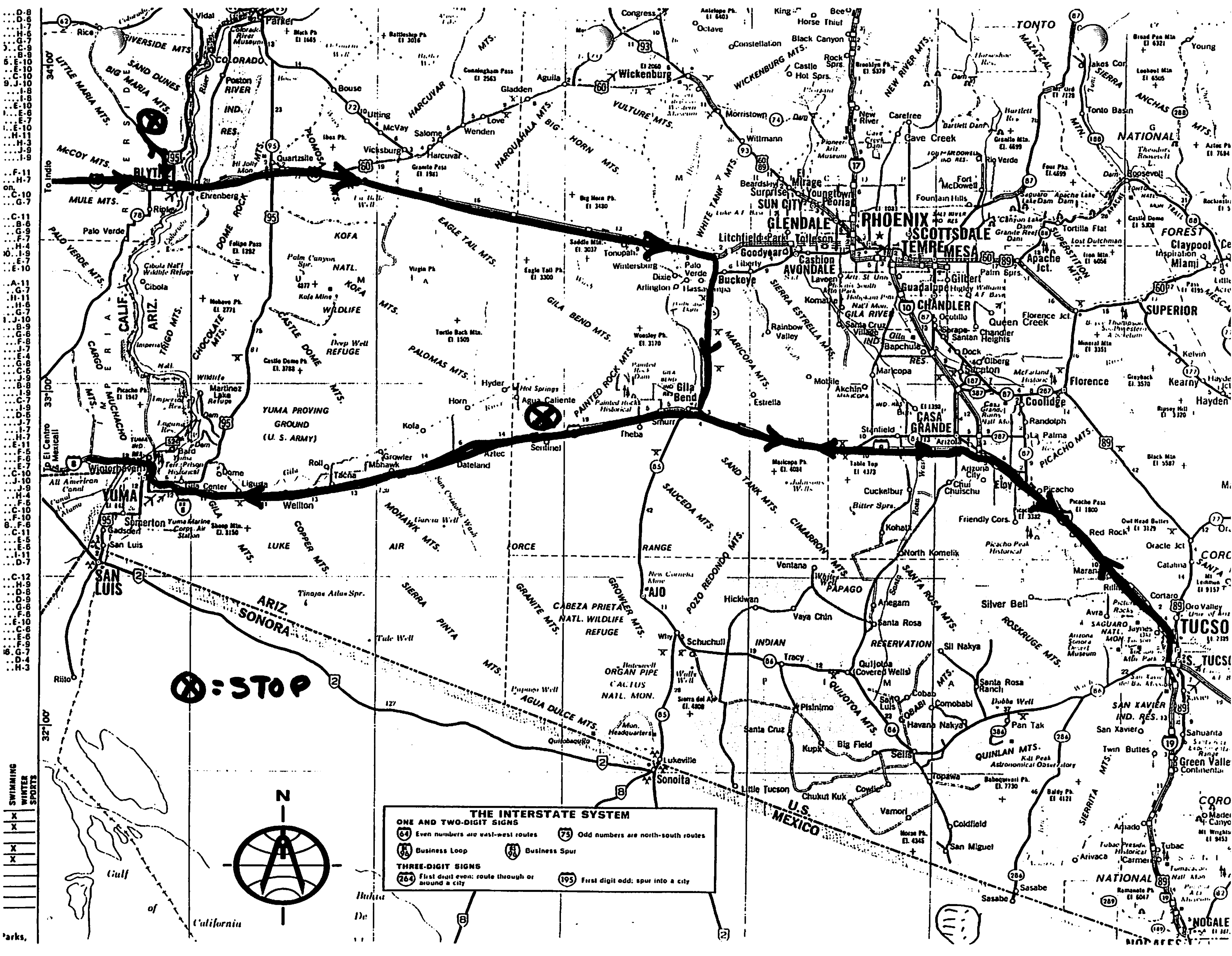

⊗ : STOP
THE INTERSTATE SYSTEM
ONE AND TWO-DIGIT SIGNS
64 Even numbers are east-west routes
75 Odd numbers are north-south routes
Business Loop
Business Spur
THREE-DIGIT SIGNS
264 First digit even: route through or around a city
195 First digit odd: spur into a city
N
To Indio
BLYTHE
Ehrenberg
Quartzsite
Vicksburg
Salome
Wenden
Aguila
Wickenburg
Tonopah
Wintersburg
Palo Verde
Buckeye
Goodyear
Avondale
Litchfield Park
Tolleson
GLENDALE
PHOENIX
SCOTTSDALE
TEMPE
MESA
CHANDLER
Gila Bend
Theba
Sentinel
Agua Caliente
Aztec
Dateland
Mohawk
Tacna
Roll
Wellton
Ligurta
YUMA
Winterhaven
Somerton
Gadsden
SAN LUIS
Stanfield
CASA GRANDE
Arizola
Eloy
Picacho
Red Rock
Marana
Rillito
Cortaro
TUCSON
AJO
Sonoita
Lukeville
Sells
Parker
Poston
Coolidge
Florence
SUPERIOR
Apache Jct.
KOFA NATL. WILDLIFE
YUMA PROVING GROUND (U. S. ARMY)
EAGLE TAIL MTS.
GILA BEND MTS.
PAINTED ROCK MTS.
MARICOPA MTS.
SAND TANK MTS.
SAUCEDA MTS.
CABEZA PRIETA NATL. WILDLIFE REFUGE
ORGAN PIPE CACTUS NATL. MON.
PAPAGO INDIAN RESERVATION
U.S. MEXICO
ARIZ. SONORA
CALIF. ARIZ.
Gulf of California

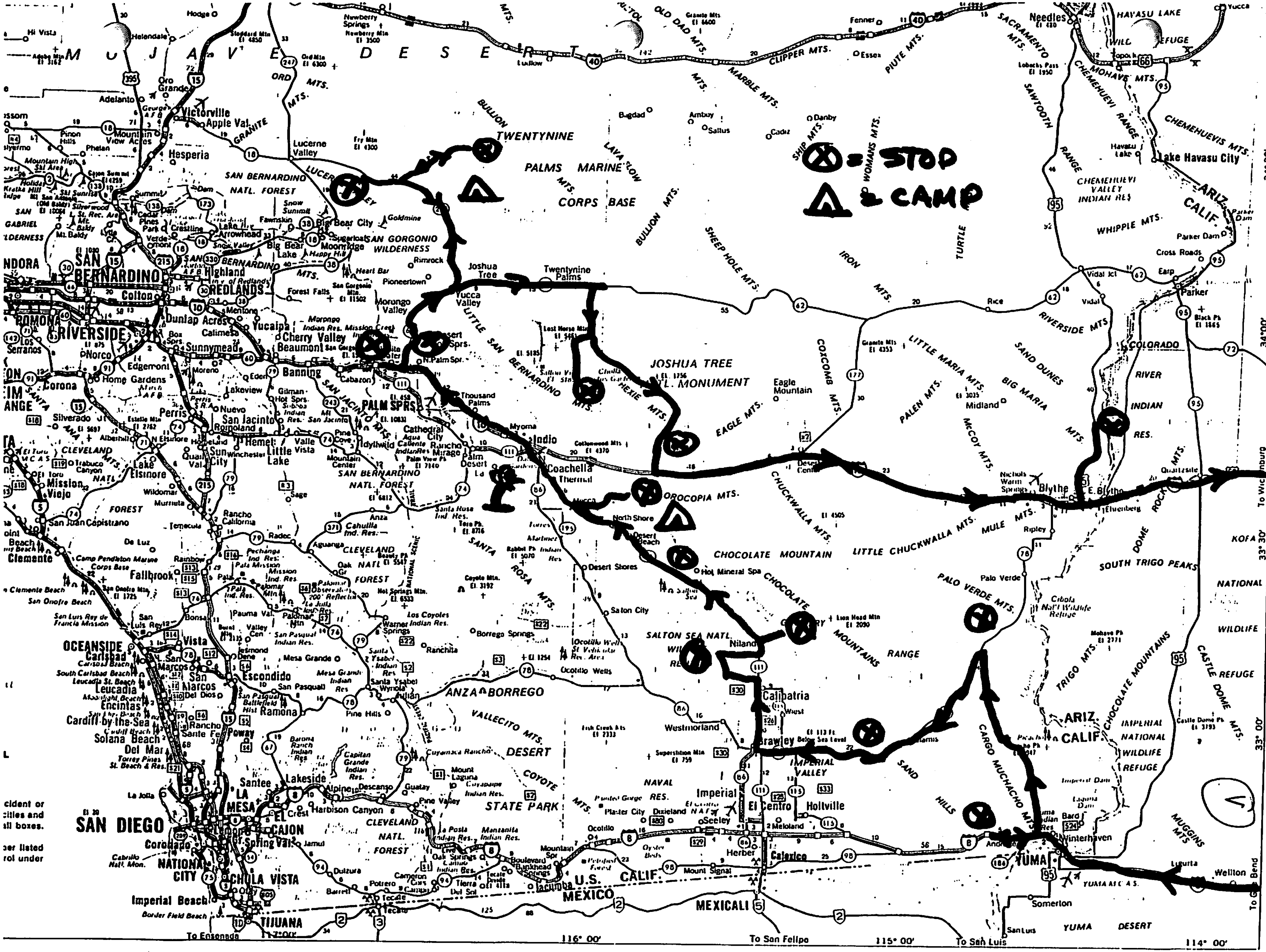

⊗ = STOP
Δ = CAMP
MOJAVE DESERT
TWENTYNINE PALMS MARINE CORPS BASE
SAN BERNARDINO NATL. FOREST
SAN GORGONIO WILDERNESS
JOSHUA TREE NATL. MONUMENT
LITTLE SAN BERNARDINO MTS.
CHOCOLATE MOUNTAIN
SALTON SEA NATL. WILDLIFE REFUGE
ANZA BORREGO DESERT STATE PARK
CLEVELAND NATL. FOREST
IMPERIAL VALLEY
SAND HILLS
CARGO MUCHACHO MTS.
CHEMEHUEVI VALLEY INDIAN RES.
COLORADO RIVER INDIAN RES.
IMPERIAL NATIONAL WILDLIFE REFUGE
KOFA NATIONAL WILDLIFE
CASTLE DOME REFUGE
YUMA DESERT
ARIZ.
CALIF.
U.S.
MEXICO
SAN DIEGO
SAN BERNARDINO
RIVERSIDE
REDLANDS
PALM SPRS.
Indio
Coachella
Blythe
Brawley
El Centro
Calexico
MEXICALI
YUMA
TIJUANA
CHULA VISTA
OCEANSIDE
Needles
Lake Havasu City
Parker
Twentynine Palms
Joshua Tree
Yucca Valley
To Wickenburg
To Gila Bend
116° 00′
115° 00′
114° 00′
34° 30′
34° 00′
33° 30′
33° 00′
5
6
7
8

(1)

PTYS 594a

PLANETARY FIELD GEOLOGY PRACTICUM

Field Trip 19-21 February 1993

K. Cyr

2

Road Logs Tucson → Casa Grande → Yuma

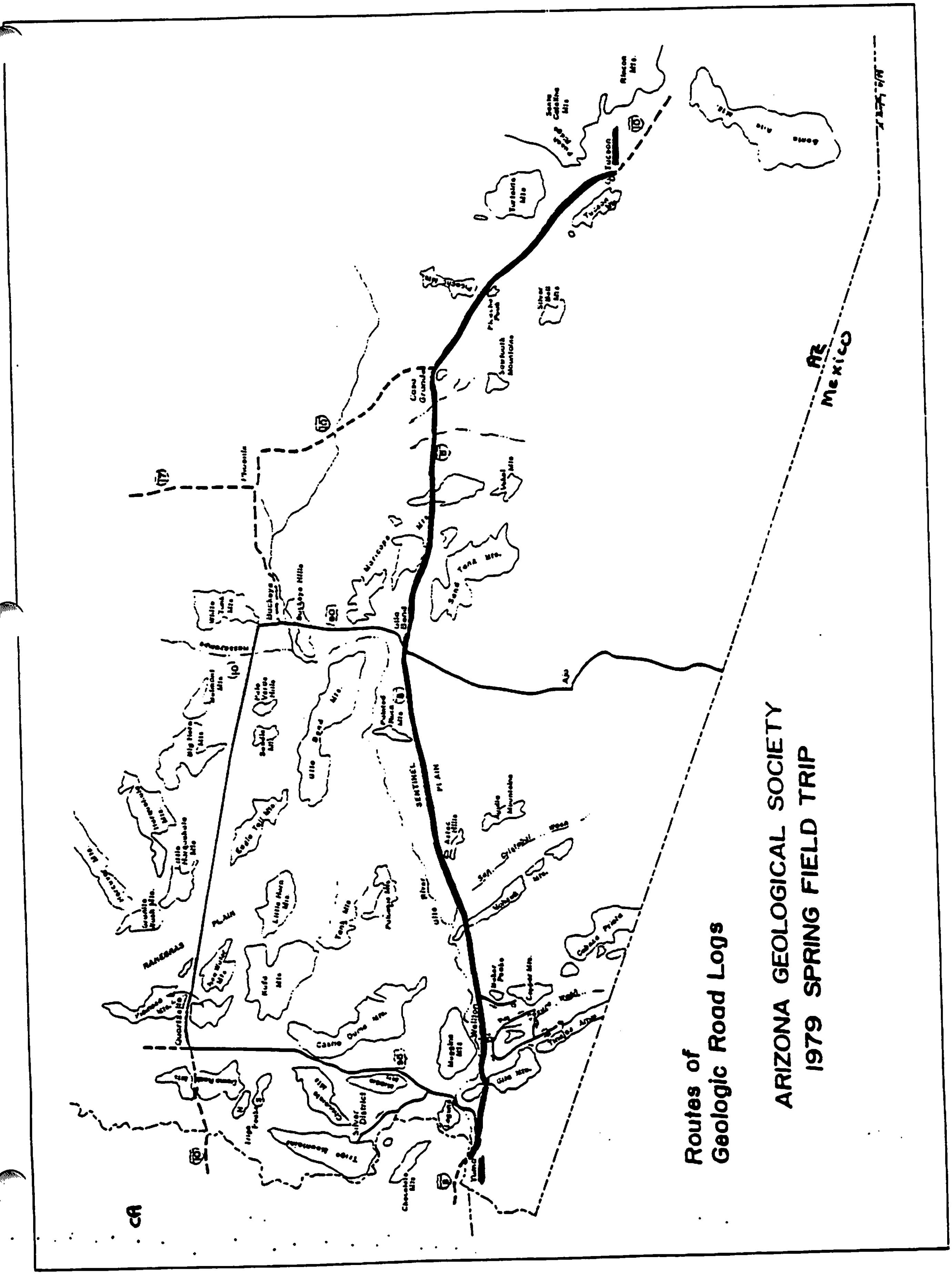

Basin & Range location:

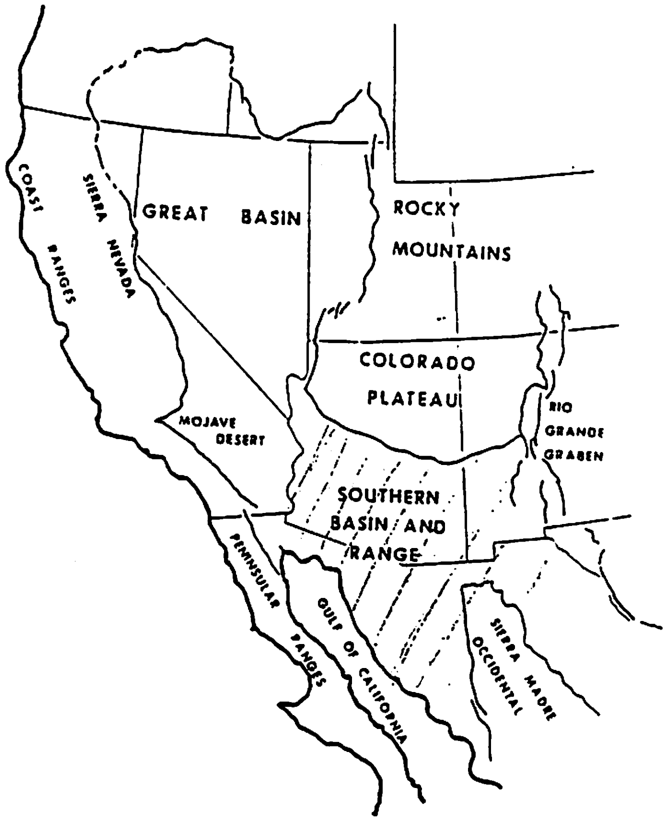

Fig. 9.2 Geologic provinces of western North America.

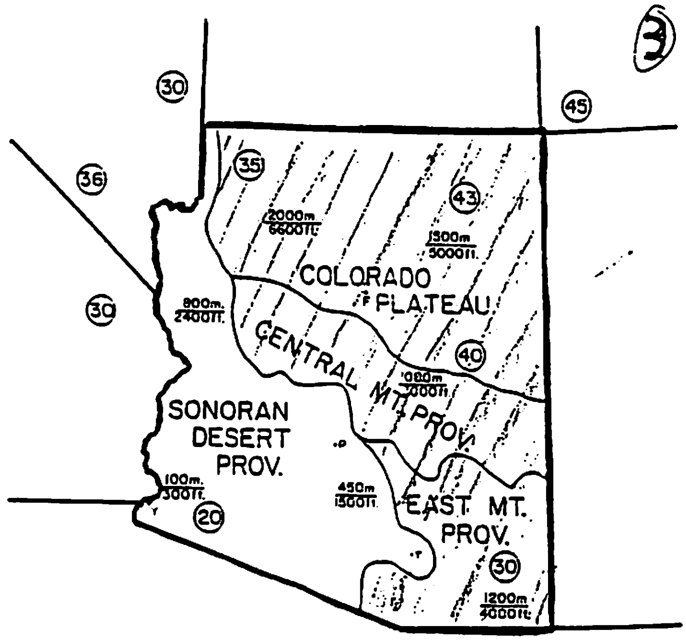

Fig. 9.3 Geologic provinces of Arizona — The Southern Basin and Range Province is divisible into 3 sub-provinces as indicated. Circled figures are crustal thicknesses in kilometers (from Pakiser, 1965; Langston and Helmberger, 1974), the underlined numbers are average elevations.

Cross Section of Basin & Range:

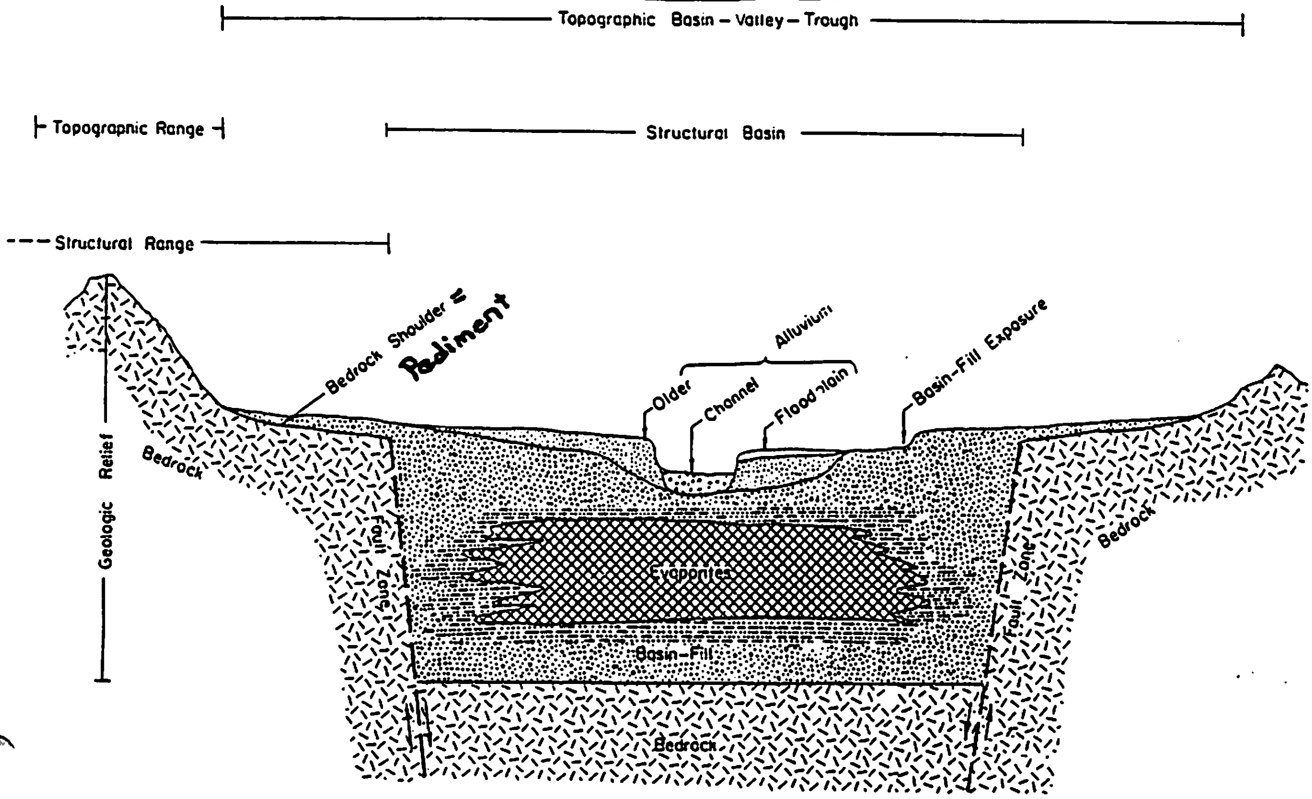

Fig. 10.2 Diagrammatic representation of features associated with range and basin structural blocks and surface topographic expression.

The Southern Basin and Range Region - Casa Grande to Yuma: Overview

Basin and Range topography = elongated mountain ranges tending NW → SE separated by broad alluvial valleys

Mountains: tilted blocks of Pre-Cambrian, Paleo-, Meso- and Cenozoic rocks plus volcanic materials; bounded by faults and severly eroded

Valleys: inter-mountain depressions in crust; subsided relative to the mountains; filled with alluvium eroded off nearby mountains

Sonoran Desert Province of the AZ Basin & Range

- valleys much broader than mountain ranges
- low valley floor elevations (~100 m @ Yuma)
- arid, sparse rainfall
- mountains: rugged, no vegetation, no talus slopes

Basin & Range started forming 30–40 my ago with the "Mid-Tertiary Orogeny"; but the modern landscape formed mostly in a later stage, 12–15 my ago.

Gila Graben

Basin & Range topography tends NW → SE

BUT Gila River flows NE → SW "against the grain"

Why? Seismic studies show Gila River flows mostly in a graben

Gila Graben = 100 mi long by 10 mi wide

Gila Bend

Believed formed due to:

(1) lava flows from Gila Bend Mtns. that deflected Gila River South from graben

(2) lava flows from Sentinel Volcanic Field that pushed Gila River North back to graben

Support: Sentinel lavas overlie Gila River sediment

Sentinel Volcanic Field

- quaternary basalt flows (1 of youngest in AZ), 1.2–3.3 my
- individual lava flows are thin (basalt has low viscosity)
  - ⇒ erupted quietly. low gas content
  - ⇒ little build up of cones

Formed <u>shield</u> volcanoes - these have an "overturned saucer" shape

- low profile cones that build up have slopes $\leq 10°$

Geology of the Chocolate Mountains and Chocolate Mt. Thrust

with your helpful host. Andrew Rivkin

Constraints

1. Orocopia Schist protolith deposited in marine-continental margin basin unconnected with subduction or island arcs
2. Schist metamorphosed at high pressure, implying subduction
3. Chocolate Mountains Thrust motion toward continent
4. Some upper-plate terranes "have southwestern North American affinities"
5. Protolith basin formed more than 80 Ma before metamorphism

Theories

1. E or NE dipping subduction zone active during late Cretaceous. W or SW directed thrusting in overriding plate, later San Andreas revives fault in other direction
2. Late Jurassic (160.9-163.2 Ma) sedimentary protolith deposited in back-arc basin between North America and island arc resting on exotic terrane
3. Deposited in intra-arc basin within Western part of Jurassic magmatic arc of Western North America, direction during closure E or NE
4. Orocopia Schist protolith deposited in deep marine basin, microcontinent plows over it, whole mess accretes onto North America from SW
5. Chocolate Mountains Thrust was engineered by ancient astronauts in order to cover up wreckage of heinous experiment being tested on Earth. Extinction of dinosaurs follows.

7

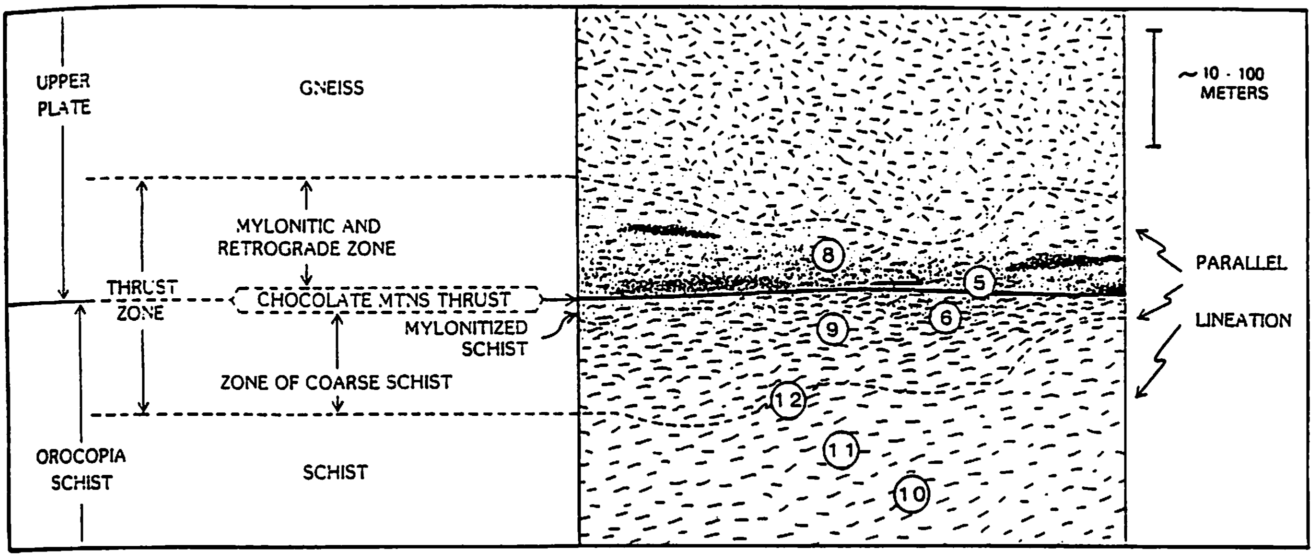

Figure 4. Schematic cross section of the Chocolate Mountains thrust zone, showing characteristic tectonic stratigraphy. The approximate position of some of the Stops within or in relation to the thrust zone is shown schematically. The thrust surface is straddled by the thrust zone, which includes all rocks of both upper and lower plate that are texturally distinct, in the field, from rocks farther above or below the thrust. Stippling represents mylonitic rocks. Dashed contacts are gradational.

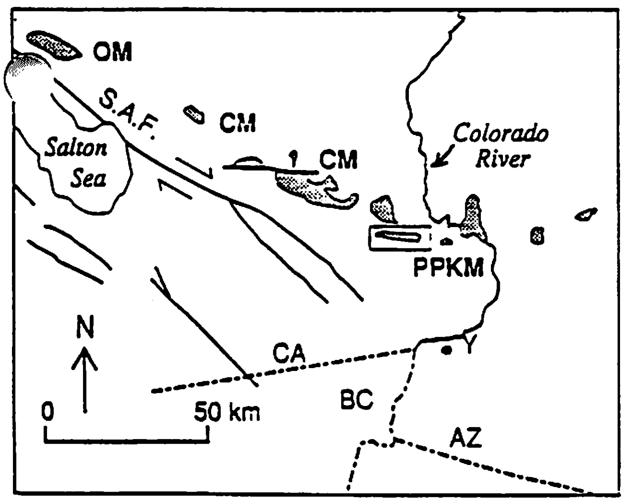

Fig. 1. Distribution of Orocopia schists (stippled) beneath the Chocolate Mountains thrust system in southeastern California. OM, Orocopia Mountains: CM, Chocolate Mountains; PPKM, Picacho-Peter Kane Mountains; AZ, Arizona; CA, California; BC, Baja California; Y, Yuma; SAF, San Andreas fault system. Adapted from Haxel and Dillon [1978] and Dillon et al. [1989]. Boxed area enlarged in Figure 2.

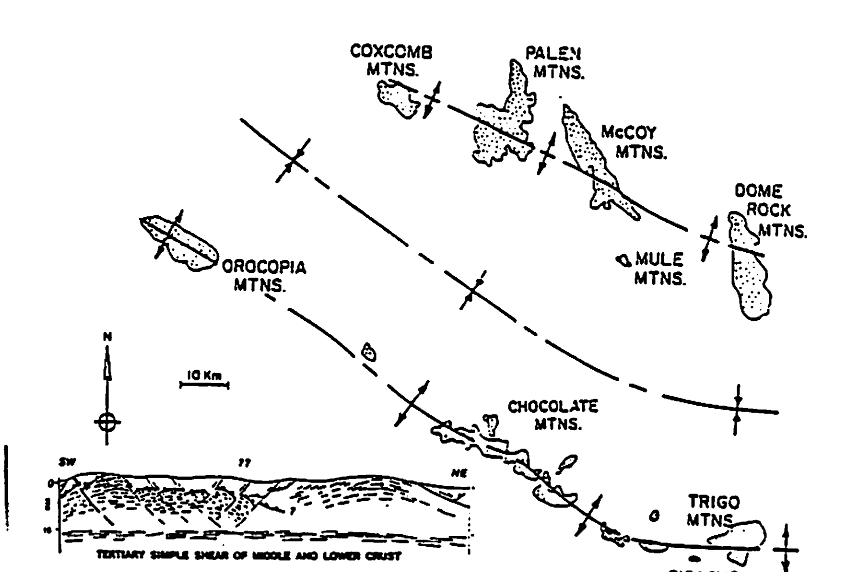

Figure 13. Diagrammatic map and cross section of some of the principal mountain ranges in southern California and western Arizona that contain thick sections of Mesozoic metaclastic rocks. Ranges on the north expose rocks considered to be the Jurassic-Cretaceous McCoy Mountains Formation. Ranges to the south expose the mostly Jurassic Orocopia Schist and Winterhaven Formation, whose relationship to the McCoy Mountains Formation is still unresolved. Seismic lines in the area indicate that the Mesozoic thrust sequence has been both extended and tilted, producing the large-scale antiforms and synforms. Prior to extension, these Mesozoic sections and their bounding thrust faults were closer together and would seem to have had a close spatial, if not genetic, relationship to each other. Near-horizontal middle- and lower-crustal reflections are thought to extend under the entire area on the basis of reprocessed industry seismic lines along portions of the cross section.

2

Rivkin

(8)

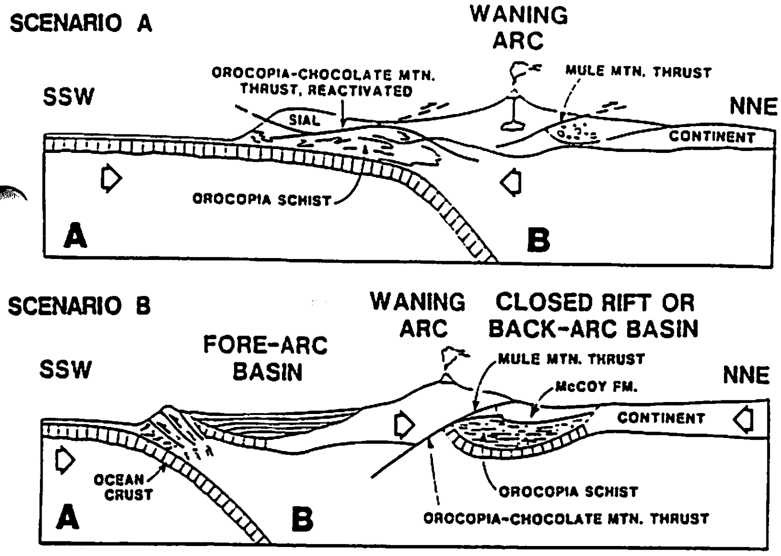

Figure 14. Interpreted plate-tectonic setting of the McCoy Mountains Formation and Orocopia Schist terranes as suggested by Crowell (1981). The McCoy Mountains terrane would appear to have been shed off both the North American continent and an arc active in Jurassic - Cretaceous time. The Orocopia Schist could be part of this same system and laterally equivalent, in part, or lower in the same tectonostratigraphic sequence as the McCoy Mountains Formation. Alternatively, the Orocopia Schist may have formed in a fore-arc position and then accreted onto North America or deformed as part of North America. The amount of strike-slip motion involved in this deformation is unknown and could easily disrupt or alter these suggested geometries. These are two of many possible scenarios and illustrate two end members for the relationship between the Chocolate Mountains thrust and the Mule Mountains thrust. Redrawn from Crowell (1981).

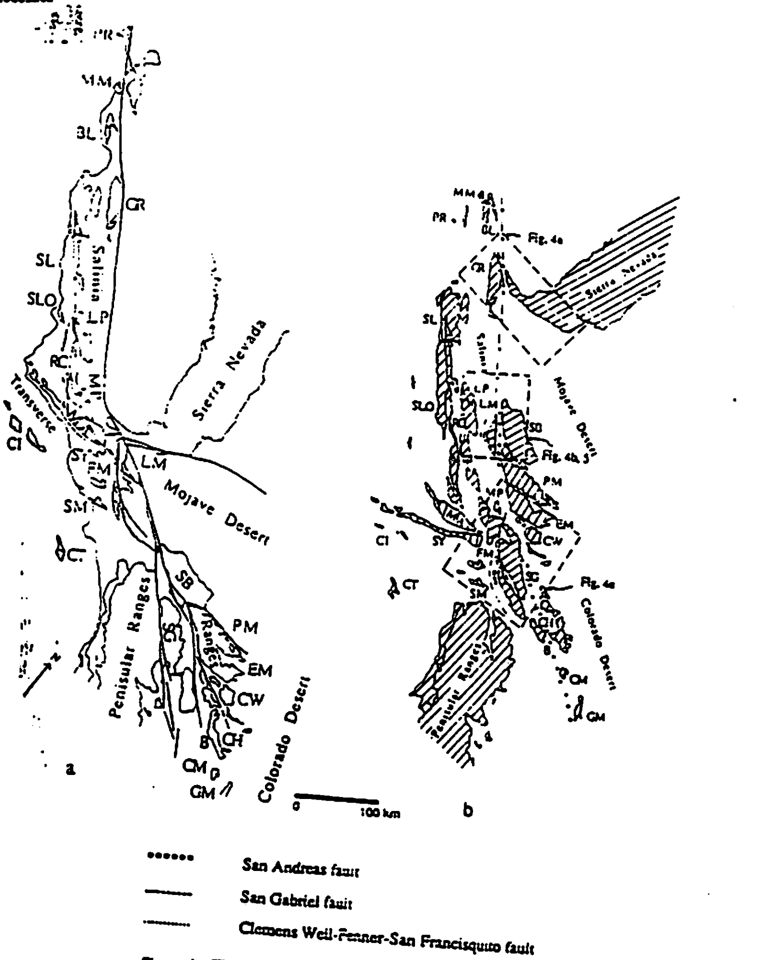

Figure 3 The San Andreas fault zone in California. *(a)* Index map showing the present-day distribution of rocks along the fault. B, Banning block; BL, Ben Lomond block; CH, Chocolate Mountains; CI, Channel Islands; CM, Cargo Muchacho Mountains; CT, Catalina Island; CW, Chuckwalla Mountains; EM, Eagle Mountains; FM, Frazier Mountain; GM, Gila Mountains; GR, Gabilan Range; LM, Liebre Mountain block; LP, La Panza Range; MA, Monte Arido block; MM, Montara Mountain; MP, Mount Pinos; PR, Point Reyes; RC, Rinconada block; SB, San Bernardino Mountains; SG, San Gabriel Mountains; SL, Santa Lucia Range; SLO, San Luis Obispo; SM, Santa Monica Mountains; SY, Santa Ynez Mountains. *(b)* The rocks reconstructed to their position prior to offset across the San Andreas system, ~20 to 22 Ma. Ruled lines show present north, to allow visualization of rotations. The future locations of various faults of the San Andreas system are shown with different symbols. See Powell (1992a) for details of the reconstruction and references for rotations.

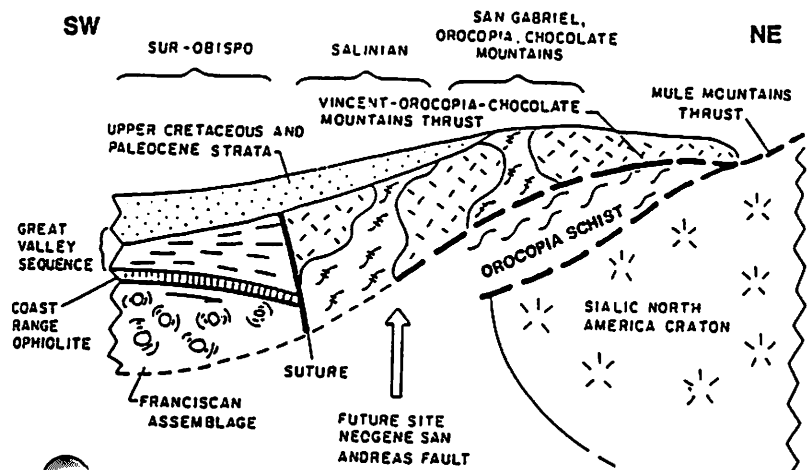

16. Diagrammatic cross section from Vedder and others (1983) showing the possible early Eocene crustal ... ucture of the Santa Lucia - Orocopia allochthon and its terrane elements. According to this model, the Orocopia Schist is sandwiched between autochthonous North America and the mostly crystalline rocks that ...it structurally above the schist. Continuation of the base of the Orocopia Schist to the southwest would supposedly put it on oceanic rocks. The reflections interpreted as the base of the schist could represent the contact of the schist with underlying North American rocks, underlying oceanic crust, or something else. Tracing these reflections to the northeast is one of the goals of the 1987-1988 CALCRUST program.

3

ALGODONES DUNE CHAIN, IMPERIAL COUNTY, CALIFORNIA
Conducted by Jim Head

The Algodones dune chain represents one of the largest (and most acessible) fields of unstabilized dunes in the United States. It is of particular interest to planetologists because the various aeloian landforms may provide analogs for martian landforms. Breed (1977) has compared the Algodones dune chain with the Hellaspontus dune field on Mars.

DESCRIPTION

The dunes overlie Cenozoic lacustrian and deltaic deposits, forming a NW-SE trending chain ~70km long and 1-8km wide (widening toward the south). The chain extends from Mammoth Wash in the north to the Colorado flood plain just south of the border (see figure). The chain consists primarily of complex, coalesced domal dunes 30-90m tall which are commonly joined into dumbbell-like forms by NE-trending saddles 300-1200m long. South of the All-American Canal, the dunes break up into sets of barachnoid forms about a kilometer across. The intradune hollows are floored by lag gravel. Individual barchans are observerd to migrate roughly 10-20m a year. Along the SW margin of the field are longitudinal dunes paralleling the chain. These are typically 5-25m high. Dunes on East Mesa (west of the chain) and along the NW margin are stabilized by vegatation. In addition, there are many small scale features present. These include small sand ripples, large granule ripples, and bush-anchored sand streamers.

WINDS

The wind regime of the dune chain is poorly characterized because 1)there are no weather stations within the field and 2)the records at the nearest stations (Imperial and El Centro to the west, Yuma to the east) show different wind directions. Winds are strongest in the spring, weakest in the fall (see figure).

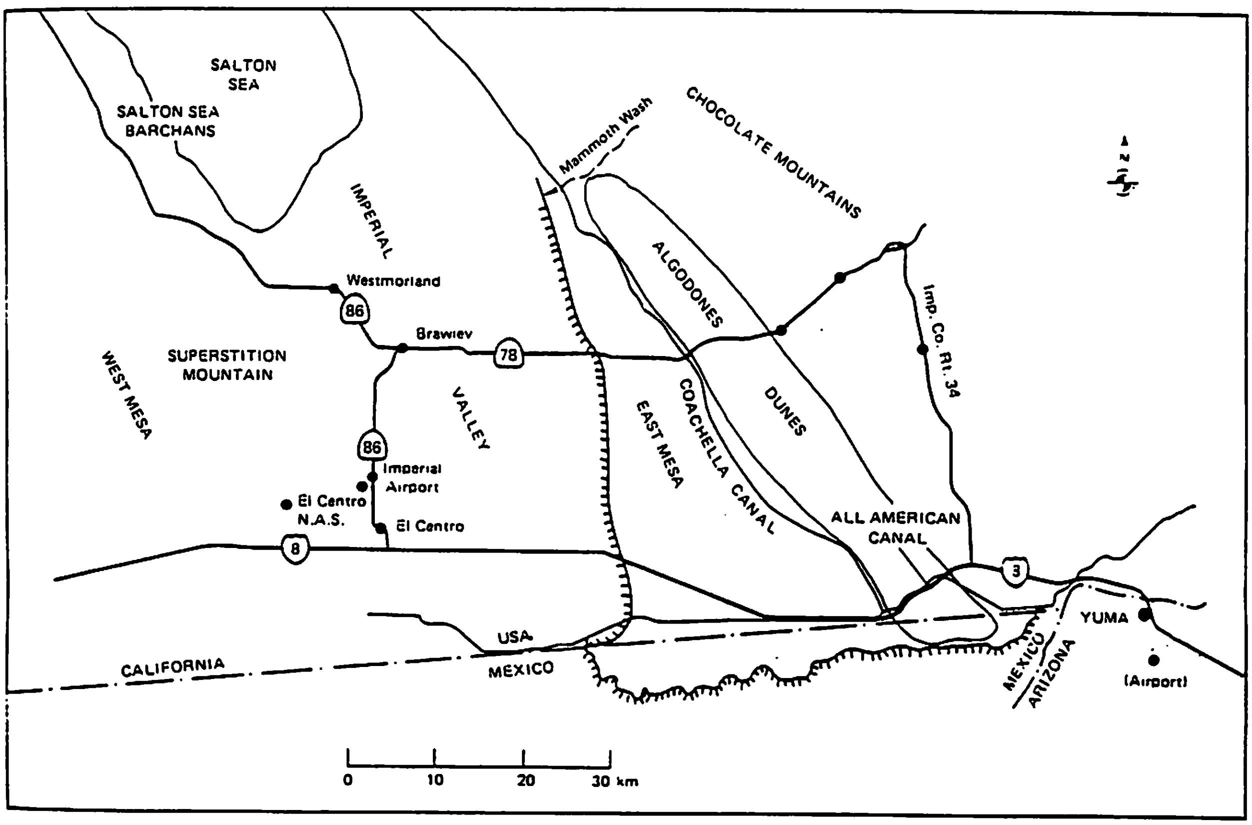

Index map of dune areas in the Imperial Valley, California.

Head

ORIGIN

The proximity of ancient Lake Chuilla shore lines to the dune field lead some workers to conclude that these beach sands are what form the dune chain, whose ultimate sources are the alluvial fans of the local mountain ranges. (The SW margin of the chain lies along the 37,000 year old lake stand. More recently, the shoreline ran along the present day west margin of East Mesa). However, van de Kamp (1973) showed that the dune sands resemble Colorado River sand and are disimilar to local alluvial fan material and the ancient beach sands. Therefore it is thought the dune field consists of Colorado River deltaic sand. The same source is cited for the Pinacate-area dune field.

	Colorado R. Sand	Basin Margin Sand
qtz	60-70%	40-50%
feld	20%	30%
chert	2%	1%

References:

Aeolian Features of Southern California (1978)

Breed, C.S. (1977) Icarus 30 326-349.

Merriam (1969) Geol. Soc. Am. Bull. 80 531-534.

van de Kamp (1973) Geol. Soc. Am. Bull. 84 827-848.

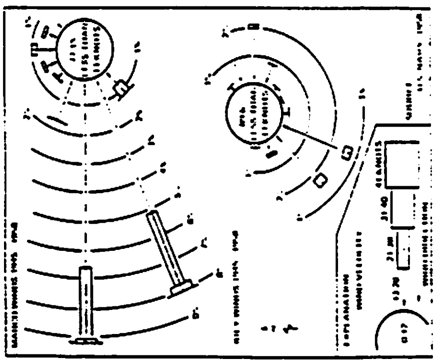

FIGURE 6.22 March and July wind roses for El Centro Naval Air Station, California (after Smith, 1970)

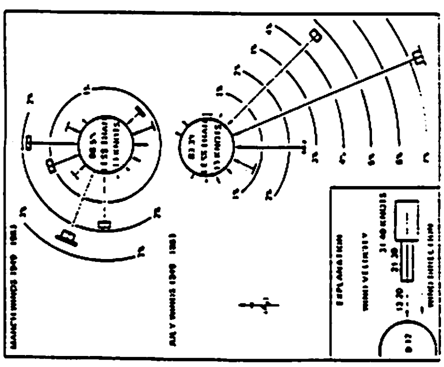

FIGURE 6.21 March and July wind roses for Yuma, Arizona, airport (after Smith, 1970)

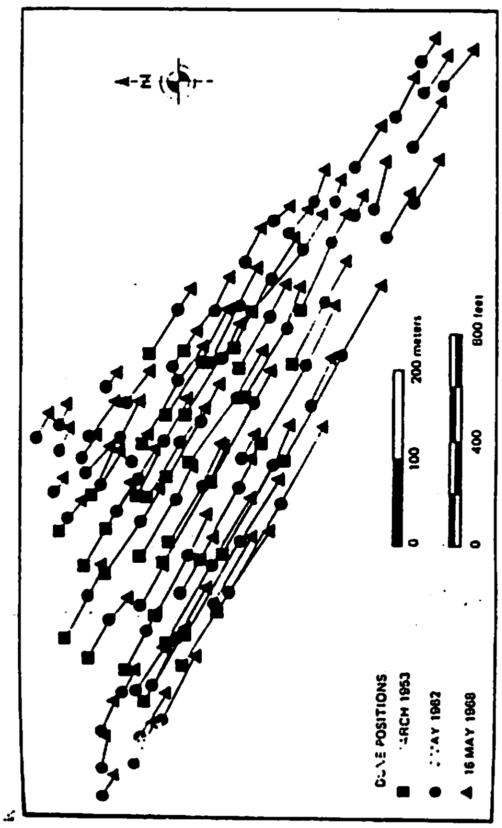

FIGURE 6-15. Map of 1953-1968 barchan migration within a field 3 km southeast of rest area on U.S. Interstate 8 (after Smith, 1970).

Palmer et al.

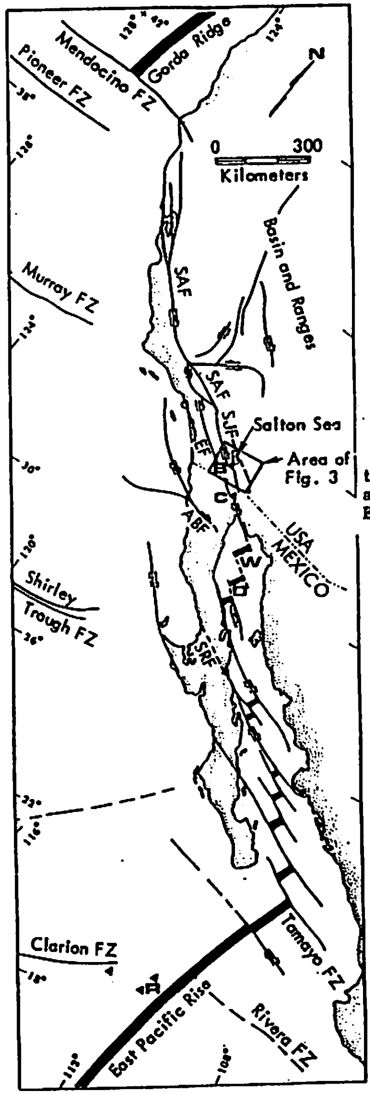

Gross tectonic environment of the Salton Trough. The Pacific Coast of North America is dominated by transform fault systems, which connect the spreading centers of the East Pacific Rise to those of the Gorda Ridge. Also shown are pull-apart basins between en echelon fault segments in the Gulf of California. Oceanic fracture zones (FZ) and continental faults (F) are solid black lines, dashed where uncertain. Other abbreviations: SAF = San Andreas Fault; EF = Elsinore Fault; SJF = San Jacinto Fault; ABF = Aqua Blanca Fault; SRF = Santa Rosalia Fault; W = Wagner Basin; D = Delfin Basin; ▲= Holocene volcanoes; B = Salton Buttes; C = Cerro Prieto; and R = Revillagigedo. (Source: Elders, et al., 1972.)

Palmer et al

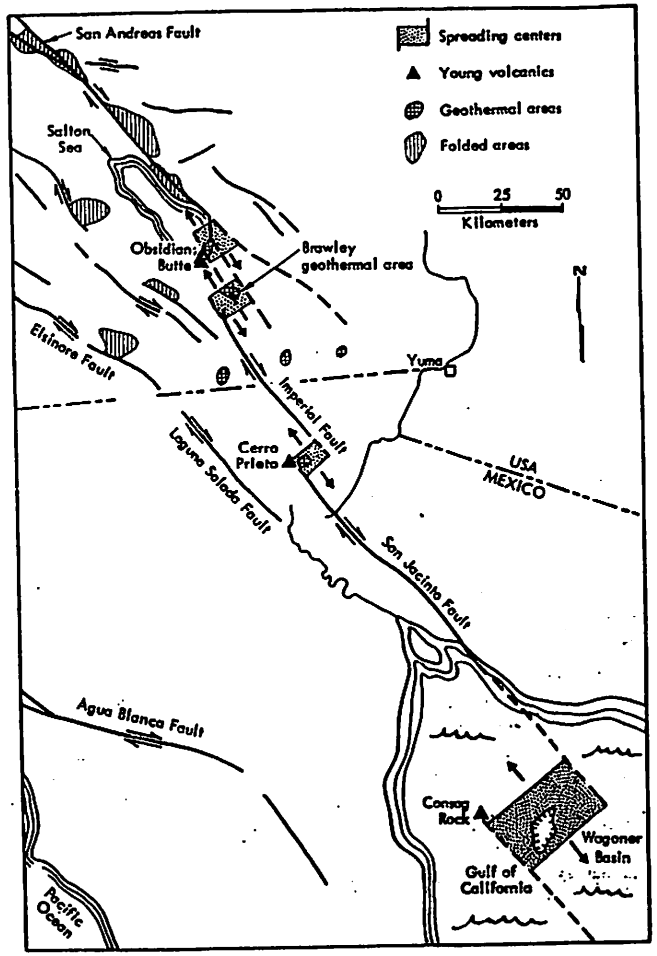

Fig. 6. Possible relationship between pull-apart basins and strike-slip faulting in the Salton Trough. Postulated "spreading centers" or tensional zones, young volcanics, geothermal areas, and zones of intense folding and compression in Tertiary sediments are indicated. (Source: Elders, et al., 1972.)

References

Palmer et al., 1975. Geothermal Development Salton Trough.

Newmark et al, 1988. Shallow Drilling in the Salton Sea Region: The Thermal Anomaly JGR 93, 13005.

Also

Elders & Sass, 1988. Salton Sea Scientific Drilling Project. JGR 93, 12953.

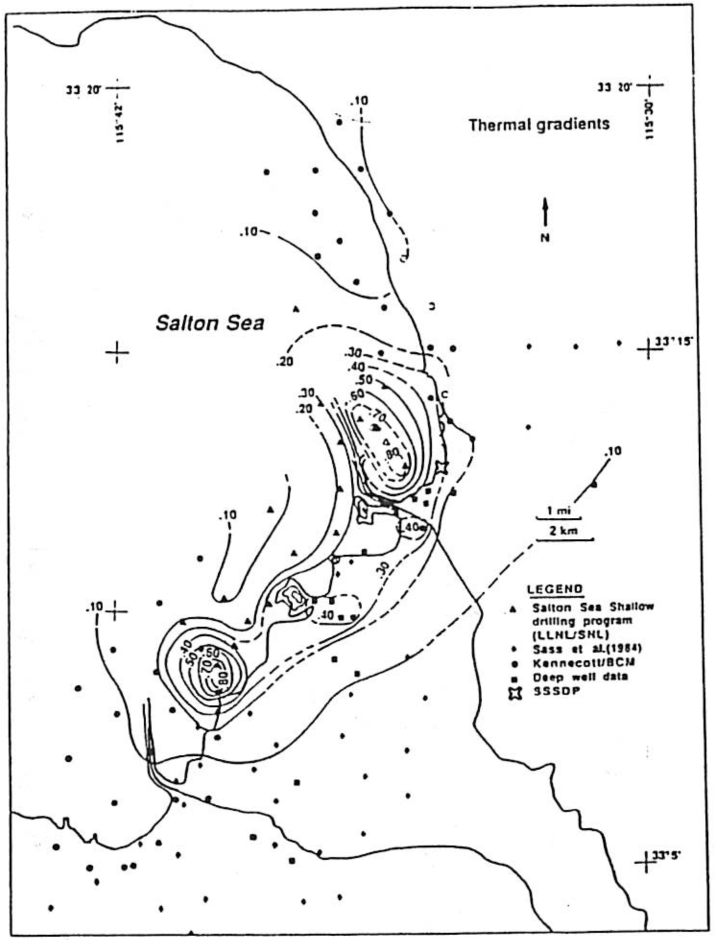

Fig. 10a. Thermal gradients in the southern Salton Sea region. Contour interval is 0.10°C/m.

Newmark et al.: Salton Sea Thermal Anomaly

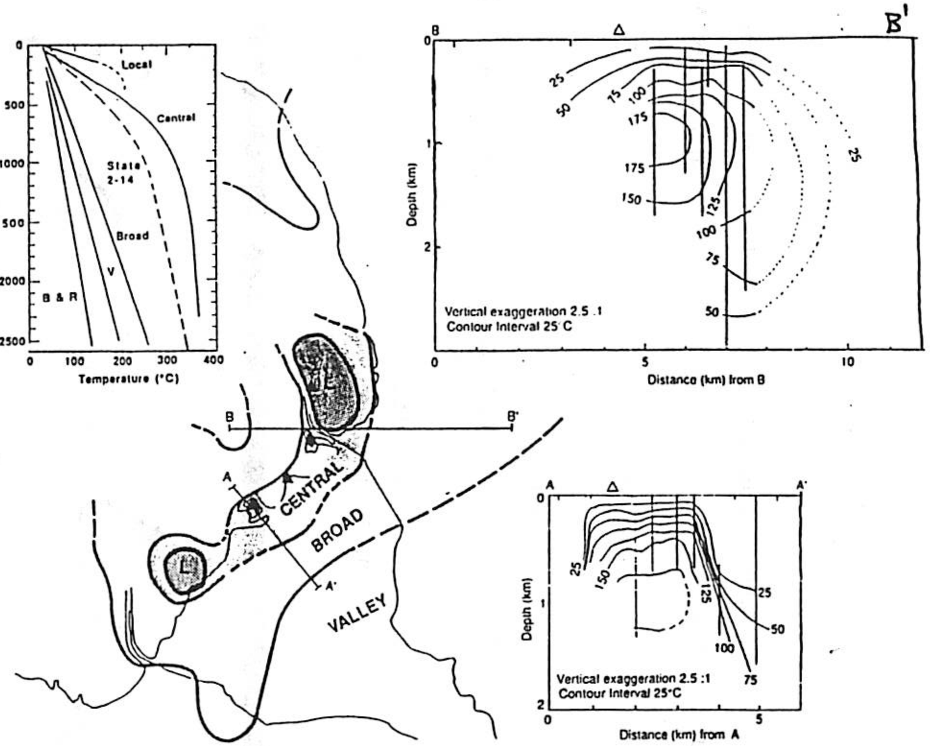

Fig. 11. Schematic representation of three scales of thermal anomalies at the Salton Sea geothermal field. The letter "L" identifies two local features bounded by the 0.5°C/m contour, the Mullet Island anomaly to the northeast and the Kornbloom Road anomaly to the southwest, which were discovered during this survey. The Central anomaly, modeled by *Kasameyer et al.* [1984], is defined to lie within the 0.3°C/m contour. The approximate boundary of the Broad anomaly is given by the 0.09°C/m contour, which extends outside the area of thermal measurements. The Local and Central anomalies have relatively sharp and well-defined boundaries, but the edge of the Broad anomaly is not well defined. Schematic temperature profiles are shown in the inset for the Local, Central, and Broad anomalies, as well as average profiles for the Imperial Valley (V) and the Basin and Range (B&R) average heat flow in sediments. Profiles A-A' and B-B' show anomalous temperatures in the axial anomaly. The anomalous temperatures were calculated from the actual temperatures by subtracting the idealized temperature profile for the broad anomalous zone, $T(z) = 23°C + 0.10\, z(m)$. Data from wells within ±2 km of the line were projected onto a vertical plane. The vertical black lines indicate portions of wells where temperatures were available. The short vertical lines indicate locations of shallow gradient wells in Tables 1 and 2, or from *Sass et al.* [1984]. The temperature profiles from these wells were extrapolated to a depth of 500 m by assuming conductive heat flow. The deep well data are from *Younker et al.* [1982]. The triangle represents the location of the volcanic arc. Section B-B' is similar to A-A' except the data were taken from wells within ±1 km from the line. Data from State 2-14 [*Sass et al.*, this issue] have been added.

Lake Cahuilla Shorelines and History

Bill Bottke, Moderator

Abstract

Intermittent NW diversion of the Colorado River into the Salton Trough during the late Quaternary is responsible for the formation of the different stands of Lake Cahuilla. The timing and duration of these stands are controlled by three factors: 1) amount and duration of river discharge, 2) evaporation, and 3) the overflow altitude of the delta threshold.

Six high stands of Lake Cahuilla, ranging from 31 to 52 m, occurred during the Pleistocene. However, the most prominent shoreline occurred at an altitude of 12 meters during the Holocene. These stands range in altitude from 10-18 m in the east to 9-20 m in the west. The difference in altitude can be attributed in part to differences in wave intensities and also to upwarping of the northern shoreline and subsidence of the southern shoreline. Four lacustral intervals have reached this level during the last 2000 years.

Lake Cahuilla Evolution (in Six Easy Steps)

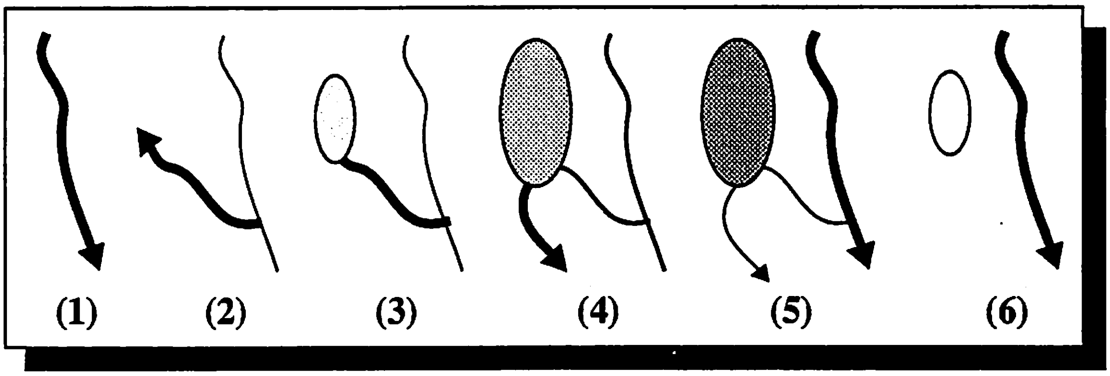

1. Major and minor channels are constantly shifting position on the Colorado River delta.
2. Occasionally, channels overflow and then cut through their natural levees towards the northwest, causing water to flow down the steeper northern gradient into the Salton Trough.
3. The lake fills rapidly at first, then more slowly as the lake's expanded surface area increases evaporation. Further cutting creates a pattern of discharge into the trough.
4. The lake fills to the overflow altitude of the delta barrier. Excess water overflows the barrier and cuts a path to the Gulf of California.
5. Prolonged diversion of the Colorado River makes the lake the site of millions of tons of silt deposition, which flattens the stream gradient. Eventually, the stream gradient to the south grows so steep that the river rediverts its discharge south down its original course.
6. The isolated lake left in the Salton Trough eventually evaporates away in ~60 years.

▲ Lake Cahuilla ▲

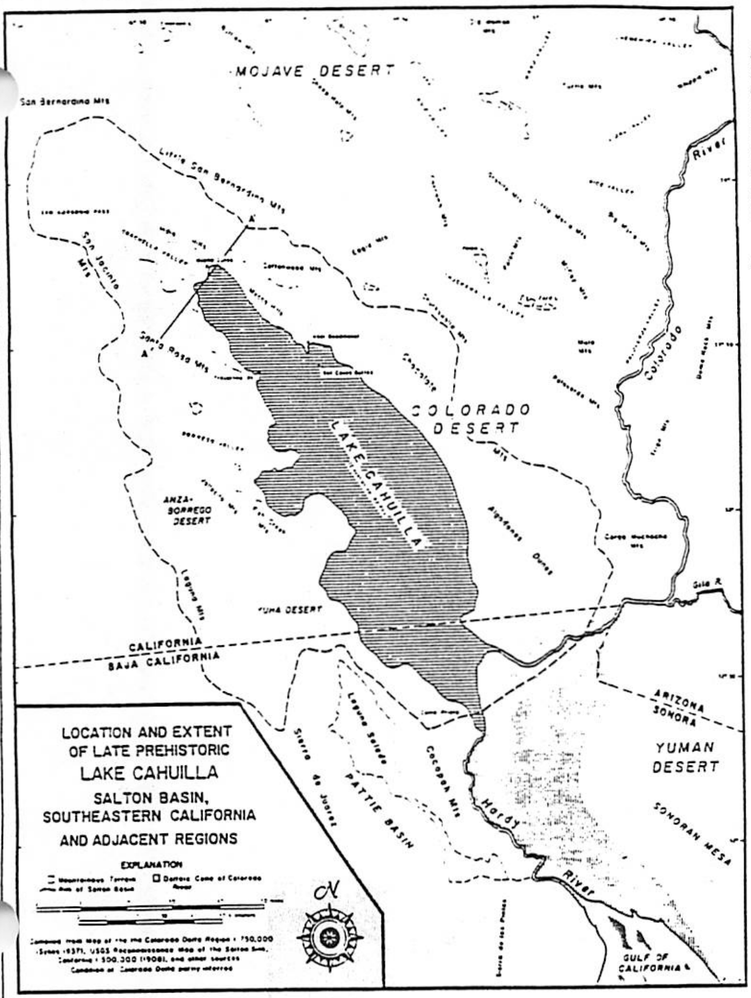

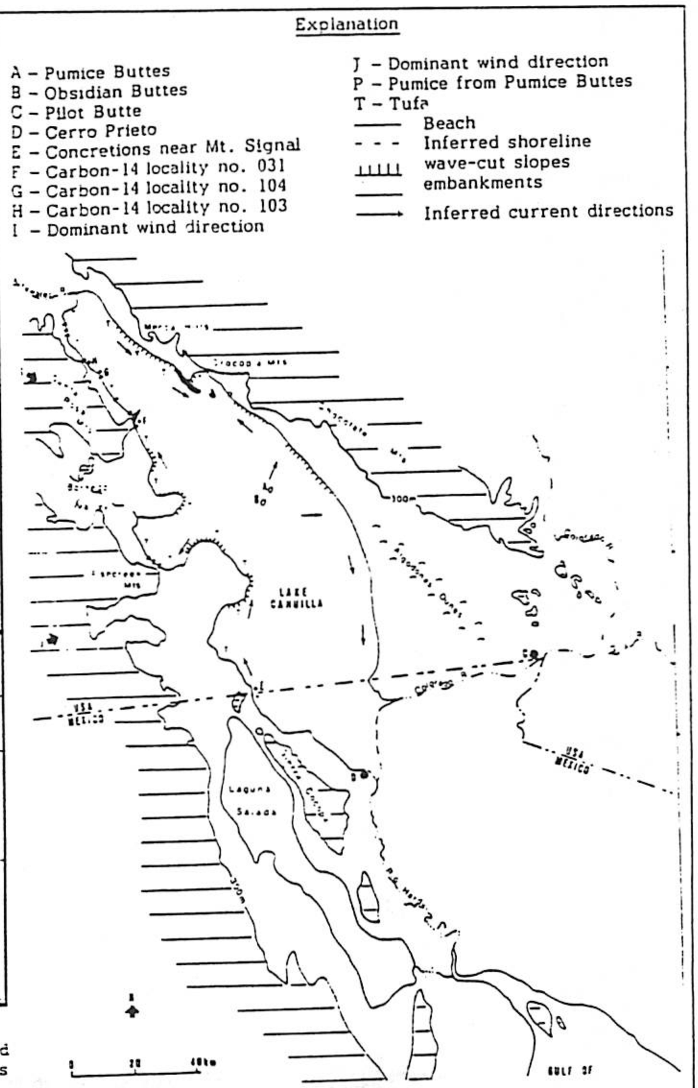

Fig. 3. The Salton Basin of southeastern California, and location and extent of late prehistoric Lake Cahuilla. Section A-A' marks location of vegetation transect shown in Fig. 13.

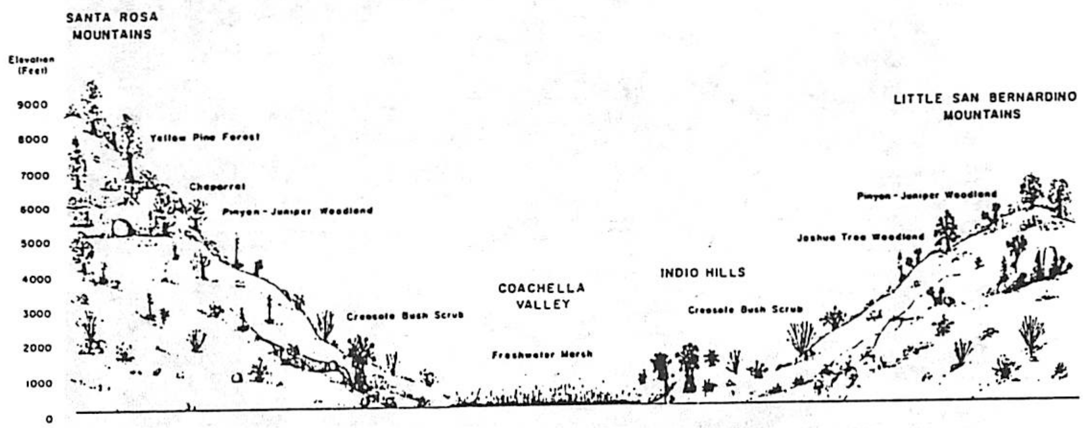

Fig. 13. Schematic and somewhat idealized cross-section of the northern portion of the Salton Basin as it existed during the last stand of Lake Cahuilla. All terrain below +42 feet elevation was inundated. Location of the transect is shown in Fig. 3.

Table 1. Relative geomorphic characteristics of the Lake Cahuilla shorelines

Characteristics	Shoreline 52-m	46-m	40-m	38-m	36-m	31-m	12-m
Desert pavement[a]	P	P	P	P	P	P	A
Desert varnish[a]	P	P	P	P	P	P	A
Soil horizon[a]							
Bt	P	P	P	P	P	P	A
Cca	P	P	P	P	P	P	A
Freshwater shell preservation[b]	D	C	C	C	C	C	Ag
Granite pebble preservation[c]	R	R	R	R	R	R	F
Beach preservation[d]	VHE	HE	HE	HE	HE	HE	SE

a. P = present; A = absent

b. D = dissolved; C = calcitic; Ag = aragonitic

c. R = rotted; F = fresh.

d. VHE = very heavily eroded; HE = heavily eroded; SE = slightly eroded.

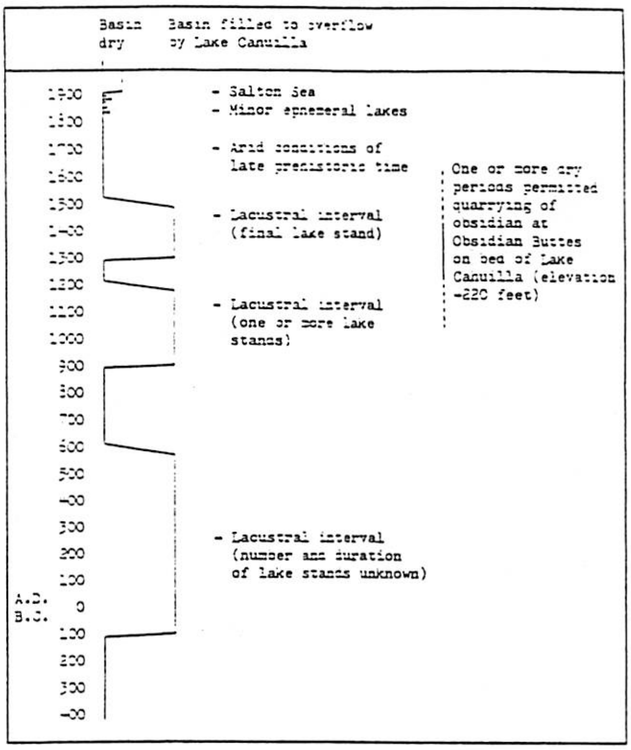

Fig. 14. Hydrologic history of the Salton Basin during the last 2000 years, as reconstructed in this text.

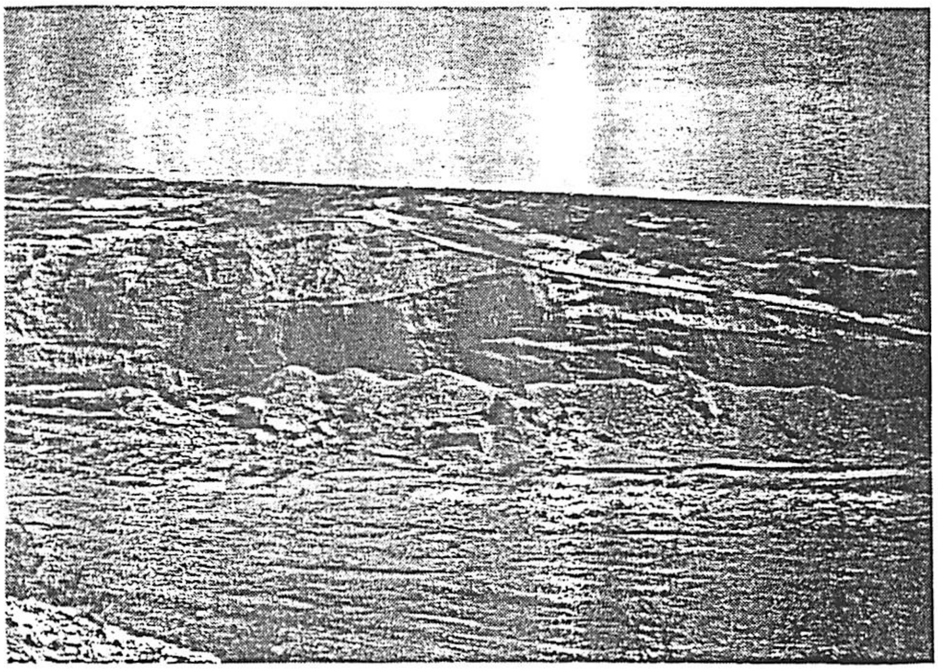

Figure 9. Late Holocene 12-meter beach in profile, eastern shoreline

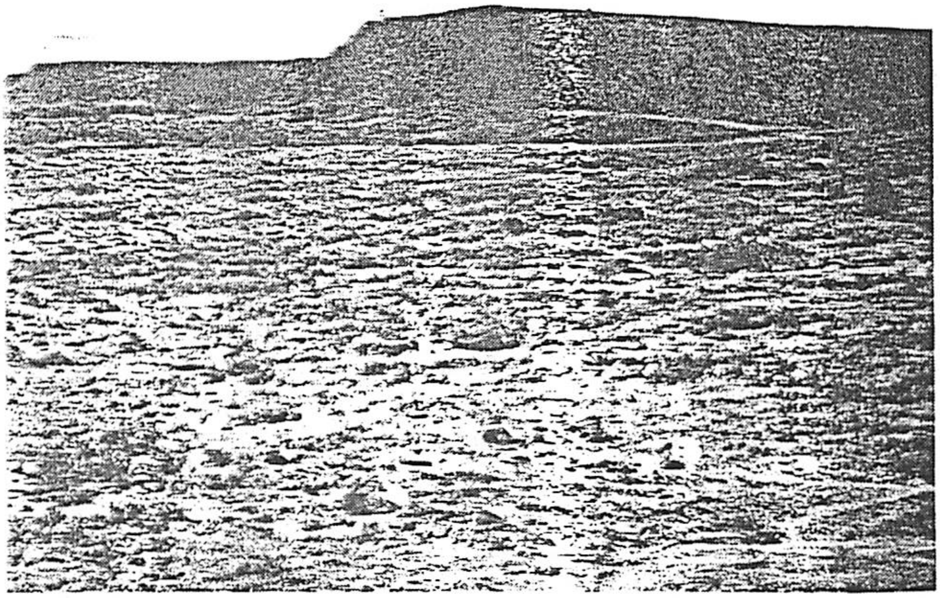

Figure 8. Wave-cut slope and bench with baymouth bar bridging a small reentrant, late Holocene 12-meter shoreline

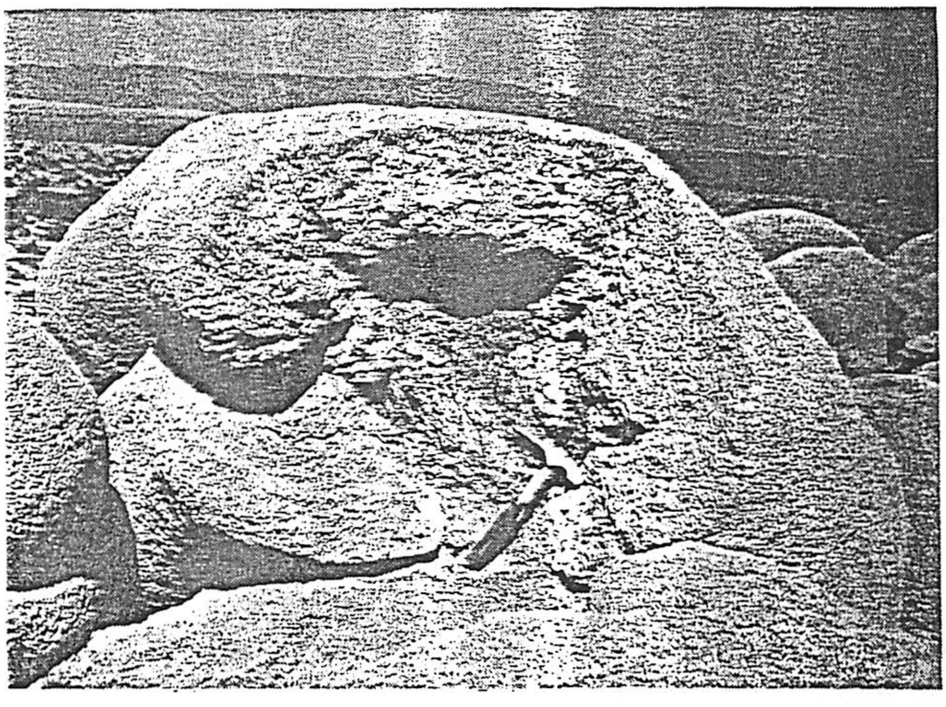

Figure 12. Coralline tufa encrusting rocks below the high-water mark (12 m) of late Holocene Lake Cahuilla, Santa Rosa Mountains,

Paleoseismology and Tectonics of the Lower Colorado Desert Southeastern California from El Centro to Indio

Compiled by Jennifer A. Grier

Background of Local Geology and Faulting

The entire Salton Basin can be considered a complex pull-apart structure resulting from the northwesterly drift of the Peninsular Ranges away from the North American Continent, accompanied by crustal spreading beneath the valley. The northwesterly movement along the San Andreas fault zone seems to be about 210 km in the past 8 to 10 million years, including several km in Holocene time (10-12,000 years).

As Baja California and the Peninsular Ranges drift northwest alongside mainland North America, local pull-apart basins, floored by thin stretched continental crust, will continue to trap sediments delivered by the Colorado River and other streams. In addition, thick sediments tend to subside as water is squeezed from them, as they compact under their own weight, and as the crust sags beneath the accumulating load.

The Basics of Paleoseismology

Paleoseismology is the recognition and characterization of past earthquakes from evidence in the geological record. Debris flow, stream deposits, marsh and peat layers and other organic sediments can be radiocarbon dated to determine their age. Further examination of fault scarps, colluvial wedges, fissure infills, upward termination of ruptures, and tilted and folded deposits above faults, with respect to these dated organic and sedimentary layers give evidence of past earthquakes.

Once the rough timing of earthquakes on a particular fault are determined, these data are analyzed to see if any earthquake trends or patterns can be found. Earthquakes along a fault may be seen to occur in groups, or perhaps occur with roughly the same magnitude each time. Relative displacement along a given fault can give the necessary information to determine these magnitudes.

Included is a diagram which illustrates how sedimentary layers and fault emplacement are used in paleoseismology to determine the date and extent of past earthquakes. The peat layers are black, and stippled units are granitic alluvial deposits. All other units are debris flows. The placement of sand dikes, fissures, scarps and bed folding relative to sediment layers show the history of displacement (i.e. earthquakes) along this fault.

Once the date of earthquakes is determined, these data are examined for trends. Included is an example from a site north of Indio. This figure shows the past 10 earthquakes at this site which appear to cluster in four groups. The dates were determined by very precise radiocarbon dating techniques, therefore the occurrence of the apparent clustering is real. Temporal clustering of large earthquakes has been observed in other regions, so its recognition at this site is not surprising. Within the clusters, intervals between earthquakes are mostly less than 100 years. The time between clusters, however, is between about 200 and 330 years.

An inspection of this pattern causes an obvious question to arise: Will the present interval complete a cluster or will it separate the end of the last cluster from the beginning of the next? Upon examination of the figure, it can be seen that five of the six intracluster intervals span less than a century, (the other interval was 134 years). This suggests that the present open interval of 135 years is probably not an intra-cluster interval, but rather a long interval separating clusters. It the latter is true, then the probability of earthquake occurrence within the next 30 years is quite low

The techniques of paleoseismology have been applied to the areas north and south of the Salton Sea to determine earthquake histories in these areas.

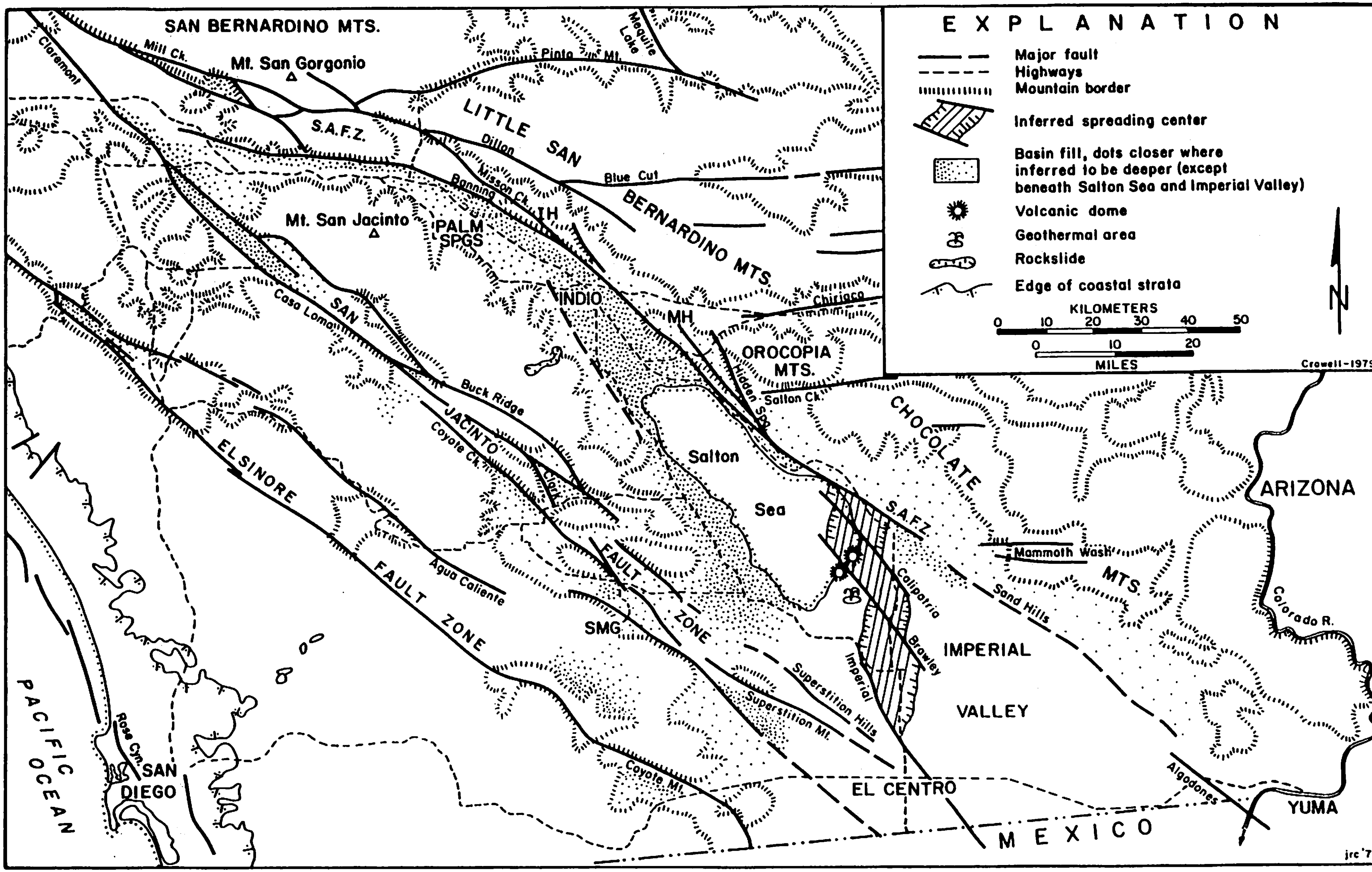

Fig. 1. Diagrammatic fault map of central Peninsular Ranges and Salton Trough region. The map shows the major faults of the San Andreas system near their juncture with the divergent plate boundary in the Salton Trough. Basin fill is indicated by stippling, and inferred active spreading centers by the line pattern SE of the Salton Sea. Abbreviations: IH, Indio Hills; MH, Mecca Hills; SMG, Split Mountain Gorge.

19

INDIO TO THE EASTERN SALTON SEA REGION (THE STOP AT SALT CREEK)

The San Andreas fault system is prominent in the Coachella Valley and along the northeast side of the Salton Sea as far south as Bat Cave Butte. The San Andreas ends at the northernmost segment of a series of spreading centers that can be traced southward all the way to the mouth of the Gulf of California and into the East Pacific Rise spreading center. There is also some evidence that there exists inactive extension of the San Andreas (the Sand Hills fault) from Bat Cave Butte toward Yuma. This southernmost 200 km of the San Andreas fault has been dormant during the historical period. Therefore, its degree of activity and potential for generating large earthquakes has remained in question.

Coachella Valley and Indio

Recent paleoseismology in the areas near and north of Indio suggests a 100 year average recurrance interval for the San Andreas fault in these areas. This value is much shorter than the 132 year interval suggested in 1984. Since many earthquake probabilities have been calculated from the larger number, it is important to reevaluate earthquake occurrence in this area. Note that 135 years have elapsed since the last major earthquake along this section of the fault.

Excavations east of Indio in 1986 provide evidence for at least four large slip events, and a slip rate of over 30 mm/yr during 1000-1700 AD. Lacustrine and fluvial beds at Indio are broken by four faults within a zone 50 m wide. At least 21 m of slip occurred across these faults between A.D. 1000 and 1700, indicating an average slip rate of at least 30 mm/yr for this period. This is in marked contrast to an average rate of about 3 mm/yr since 1700 and 2 mm/yr since 1949. This and other data show that the San Andreas fault at Indio has experienced a decrease both in average slip rate and size of slip events during the past millennium, and that this section of fault has shown to produce a large earthquake every 2-3 centuries.

Eastern Salton Sea

The creation of the Salton Sea by accidental diversion of the waters of the Colorado River into the Imperial and Coachella valleys in 1905 has provided an opportunity for determination of the average rate of slip on the San Andreas fault during the past 80 years. Before the river could be rerouted, the surface of the Salton Sea had risen to an elevation of 60 m below sea level. This caused the lake to flood the channel of Salt Creek and deposit lacustrine sediment across the fault trace there. Offset of the lacustrine bed reveals the average slip rate of the fault during the twentieth century. Pleistocene and Plio-Pleistocene units here commonly display folds and minor faults and steep to moderate dips. Locally overlying these rocks, within the embayment of Salt Creek, are fluvial, aeolian and lacustrine gravel, sand and chips predominantly of Holocene age. Exposures of the young sediments revealed the fault strands. From observations of the offset of deposits, an average slip rate of 2.0 mm/yr. was calculated.

Some Conclusions

This and further evidence suggests that these portions of the San Andreas from Indio to the Salt Creek have been slipping at low rates throughout the past three centuries. Near the Salton Sea the modern rate of 4 mm/yr as measured by creepmeters is similar to an average rate of about 2 mm/yr which spans the twentieth century, and to a 3 mm/yr rate, which spans the past three centuries. The reason for long-term, low-level creep is unclear. It is possible that slow, quasi-continuous aseismic slip occurs here because of the high pore pressures in the coarse sediments that abut the fault. High pore pressures would reduce the effective normal stress on the fault and thus reduce its strength. At greater depths, where consolidated and relatively impermeable crystalline rocks abut the fault, the strength of the fault would be higher, and the fault plane would be locked between large earthquakes. The presence of the locked patch prevents the weak upper few kilometers of the fault from slipping at rates closer to the long-term rate of slip of about 24 mm/yr. This implies that low-level creep is not a short-term precursor to major seismic failure in this area. This also implies that these sections of the fault are currently locked and slip primarily during great earthquakes every 2-3 centuries.

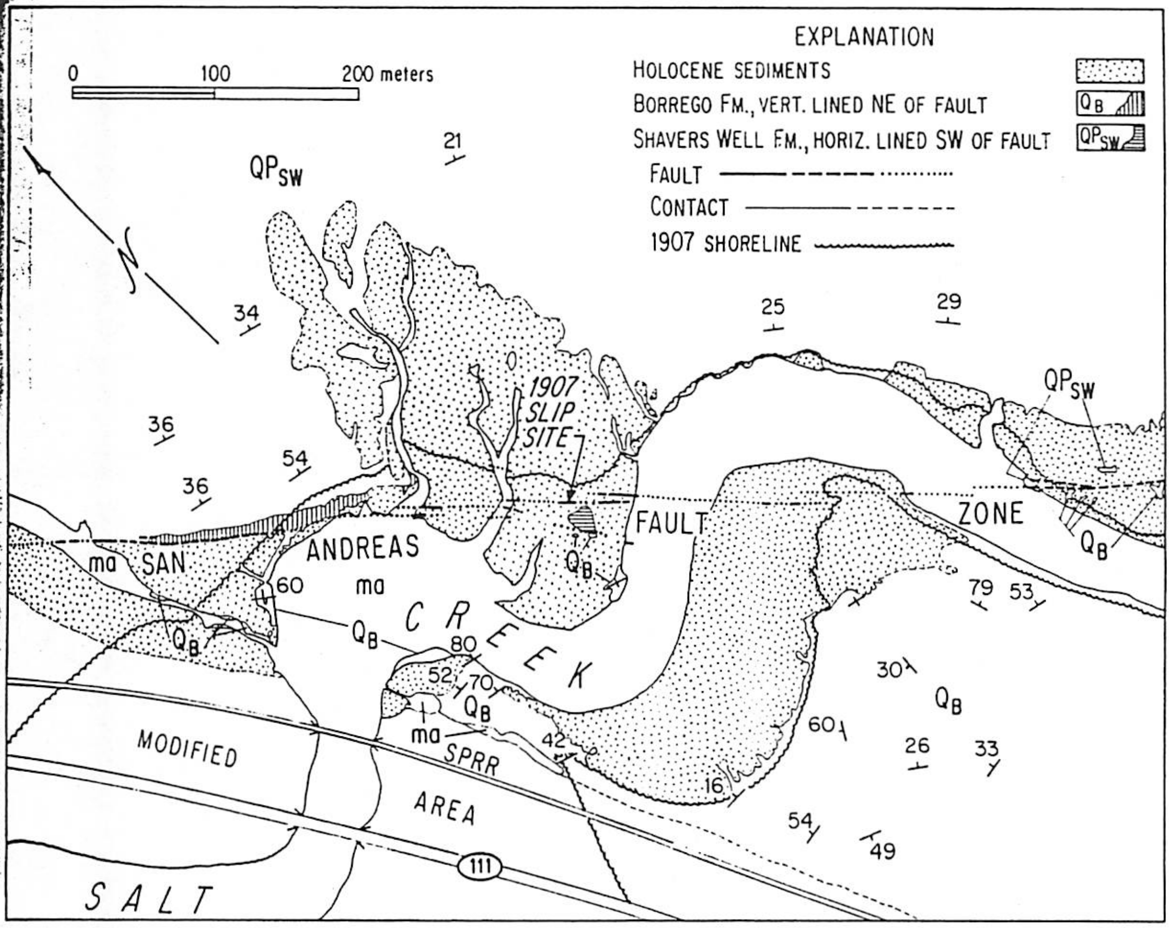

Fig. 9. Geological map of the lower reach of the Salt Creek drainage. The waters of the Salton Sea invaded the drainage in 1907 and left lacustrine sediment that has been offset subsequently by the San Andreas fault.

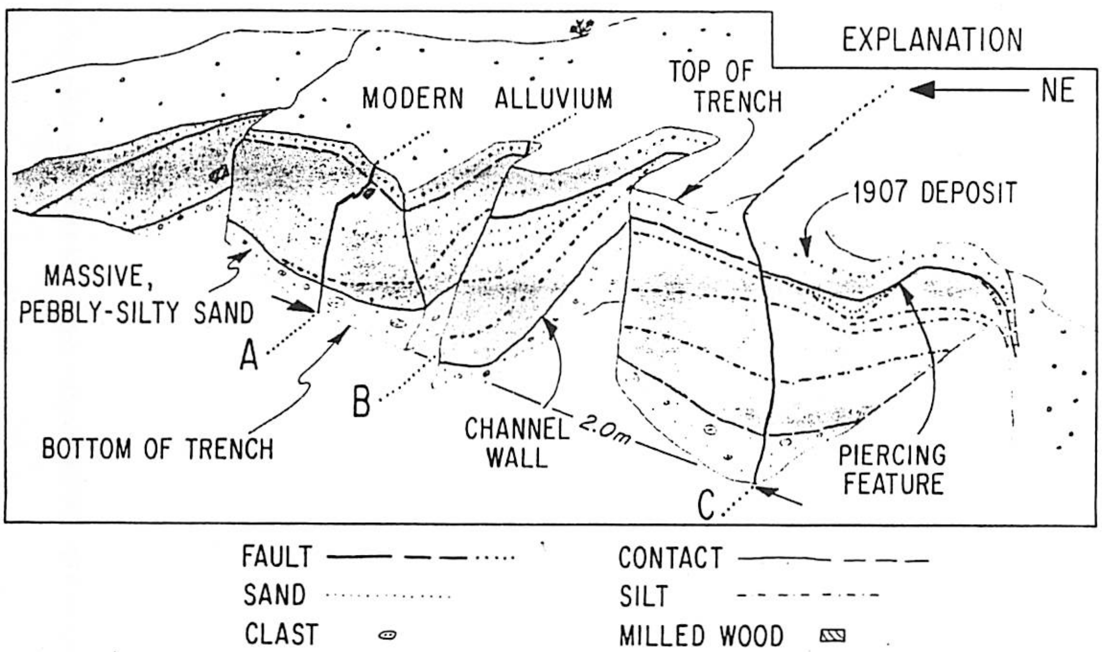

Fig. 10. Sketch (from photograph) of channel deposits excavated near the 1907-high-water level of the Salton Sea. View is to the east. The channel flowed from the upper left to the lower right. Lacustrine sand that filled the channel in 1907 was supplied primarily from the southeast.

Griev

22

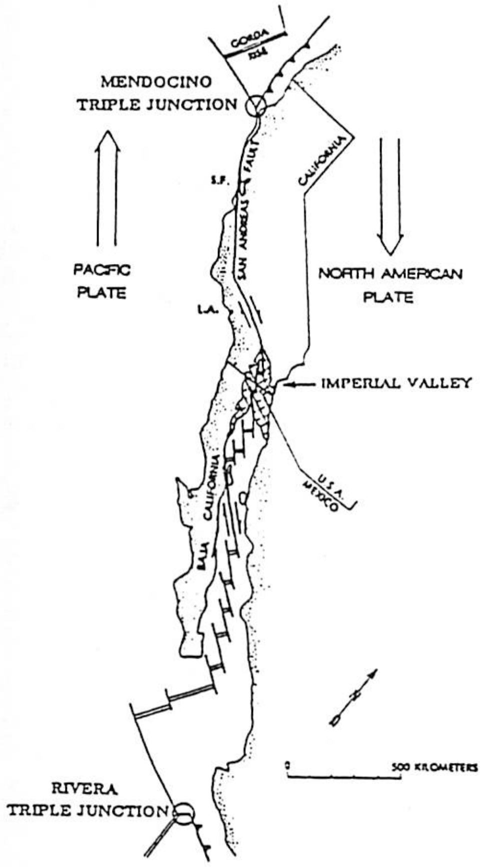

Fig. 1. The Salton Trough (hatch pattern) is a transition zone between crustal spreading in the Gulf of California and right-lateral transform motion along the San Andreas fault. The Imperial Valley is that portion of the Salton Trough north of the U.S.-Mexico border and south of the Salton Sea. Abbreviations are S.F., San Francisco; L.A., Los Angeles. Map modified from *Lachenbruch et al.* [1985].

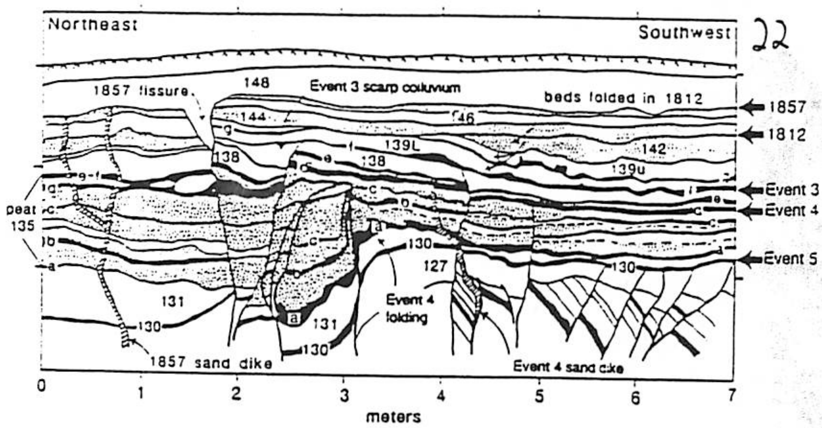

Fig. 4. Composite log of Swarthout Creek exposures at northwest corner of site showing deformation on the main fault zone associated with past five earthquakes. Fault strands shown by heavy lines. Peat layers are black, stippled units are granitic alluvial deposits. All other units are debris flows. Numbers shown for units mentioned in text. Earthquake horizons are shown by broad arrows.

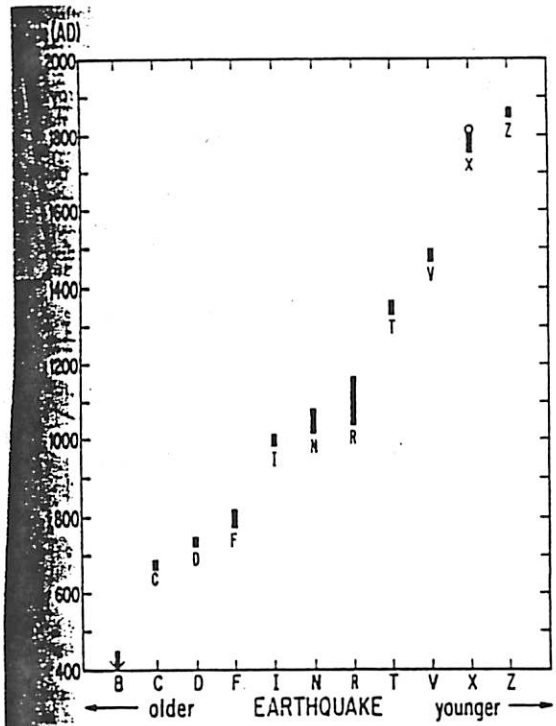

...163. New estimates of the dates for earthquakes recorded in the ...nts at Pallett Creek. Bars give 95% confidence intervals. Open ...bar of event X indicates preferred date of A.D. 1812.

REFERENCES:

Fumal, T.E., Pezzopane, S.K., Weldon II, R.J., and Schwartz D.P. *A 100-Year Average Recurrence Interval for the San Andreas Fault at Wrihtwood, California.* Science. Vol. 259. January 8, 1993. Pp 199-203.

Johnson, C.E., and Hutton, L. K.. *A tectonic Model for the Imperial Valley and its Relation to Seismic Risk on the Soutern San Andreas Fault. (abstr).* EOS. Vol. 67, No. 44, November 4, 1986. Pp. 1200.

Larsen, Shawn, and Reilinger, Robert. *Age Constraints for the Present Fault Configuration in the Imperial Valley, California: Evidence for Northwestward Propagation of the Gulf of California Rift System.* JGR. Voll. 96, Pp 10,339-10,346. June 10, 1991.

Norris, Robert M., Webb, Robert W. **Geology of California.** Second Edition. John Wiley and Sons, Inc. 1990.

Sieh, Kerry; Williams, Patrick. *Behavior of the Southernmost San Andreas Fault During the Past 300 Years.* JGR. Vol 95, Pp 6629-6645, May 10, 1990.

Sieh, Kerry; Stuiver, Minze; Brillinger, David. *A More Precise Chronology of Earthquakes Produced by the San Andreas Fault in Southern California.* JGR. Vol. 94, Pp 603-623. January 10, 1989.

Sieh, Kerry. *Slip Rate Across the San Andreas Fault and Prehistoric Earthquakes at Indio, California. (abtr).* EOS. Vol. 67, No. 44, Novernmber 4, 1986. Pp 1200.

Thanks to Dr. Phil Pearthree, Arizona Geological Survey.

Ellen Howell

23

Irrigation in the Imperial Valley or The Salton Sea Accident

Outline of events

1850	Oliver Wozencraft proposes Colorado Desert can be irrigated
1892	Charles Rockwood rediscovers irrigation plan
1900	George Chaffey finances and leads project
1901	Water reaches Imperial Valley
Feb 1902	Rockwood regains control from Chaffey
1903	Winter Droughts limit water to Valley: CA Development Co. in trouble
Sep 1904	Mexican cut made to bypass silted canal
Mar 1905	First attempt to close the break fails
Apr 1905	Southern Pacific RR takes over the Ca Development Co.
Jun 1905	Closure abandonded after 2 more tries fail: Salton Sea starts to fill
Dec 1905	Mexican Government finally approves gate plans
Apr 1906	Rockwood gate construction completed: Harry Cory takes over
Jul 1906	Begin construction on a railroad to site of river break
Oct 1906	Rockwood gate fails; Break now half-mile wide. all Colorado River flowing to Salton Sea:
Nov 1906	Rock Dams constructed. break closed: Salton Sea stops filling
Dec 5 1906	Gila flood causes new break: Salton Sea filling again
Dec 20 1906	US Government promises to fund SPRR to close break
Feb 10 1907	Rock Dams finished, river diverted.
1907-1908	Extensive levee system put into place
1915	Dam built at Yuma to raise water level illegally
1916-1926	Removable Dam system used successfully during low water
1928	Boulder Canyon Act approved. work started on Boulder Dam 1930.
1935	Boulder Dam completed, providing flood and silt control for Colorado River

Howell

24

MAP OF THE IMPERIAL IRRIGATION DISTRICT AND LANDS IRRIGABLE BY GRAVITY FROM THE IMPERIAL CANAL SYSTEM

SCALE IN MILES.

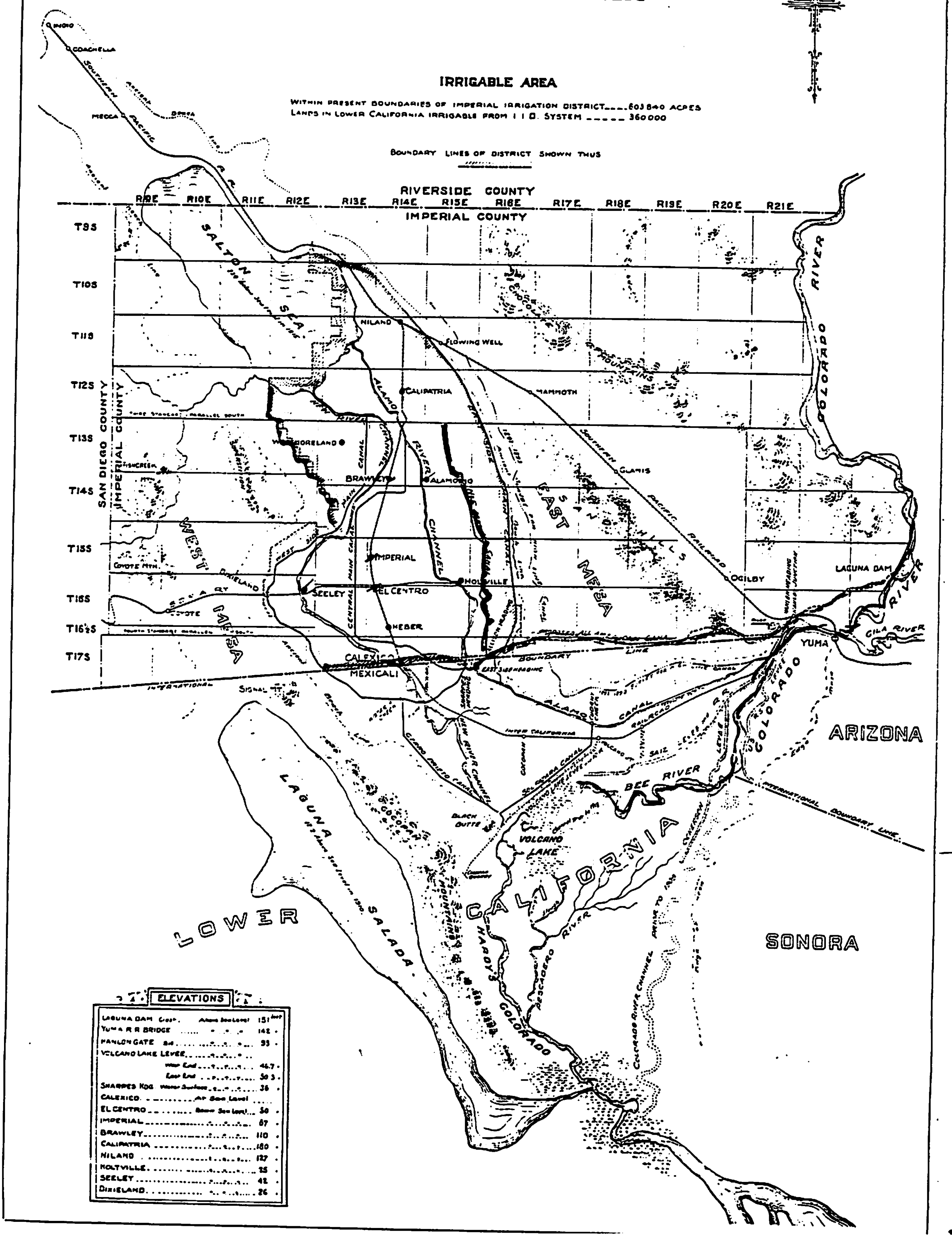

Howell

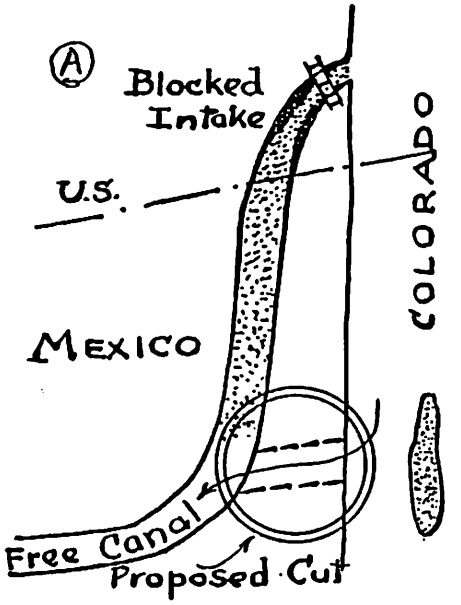

Heber's Mexican intake

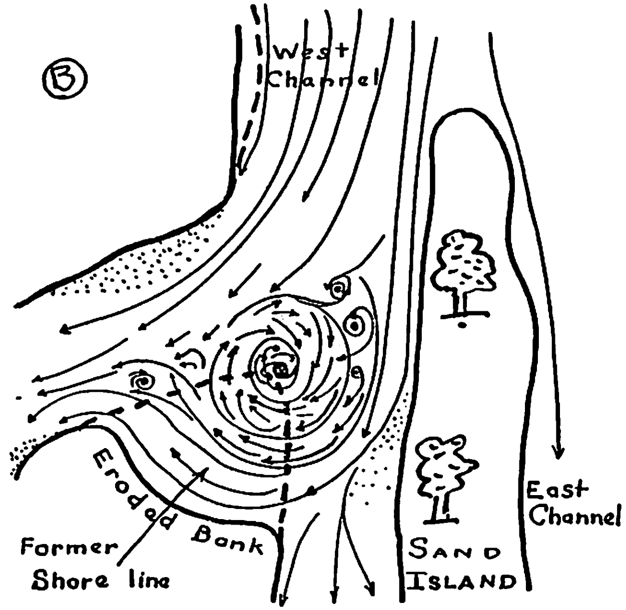

The Whirlpool that diverted a River

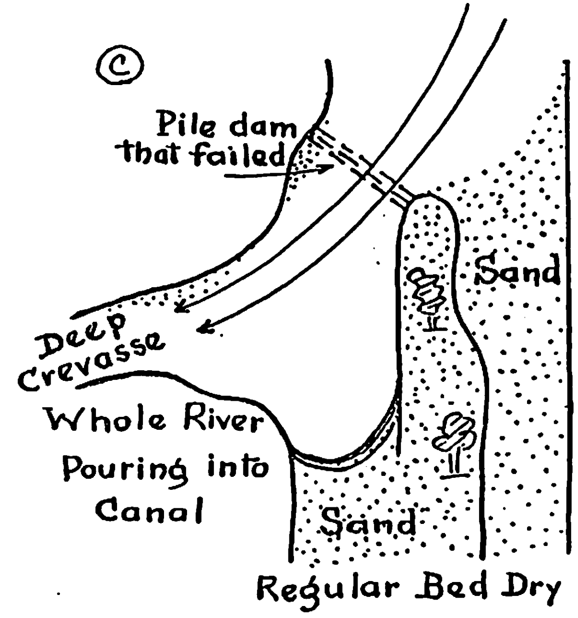

The first attempt fails

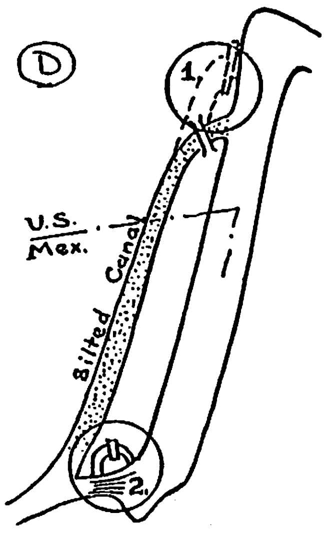

Randolph's two-gate plan

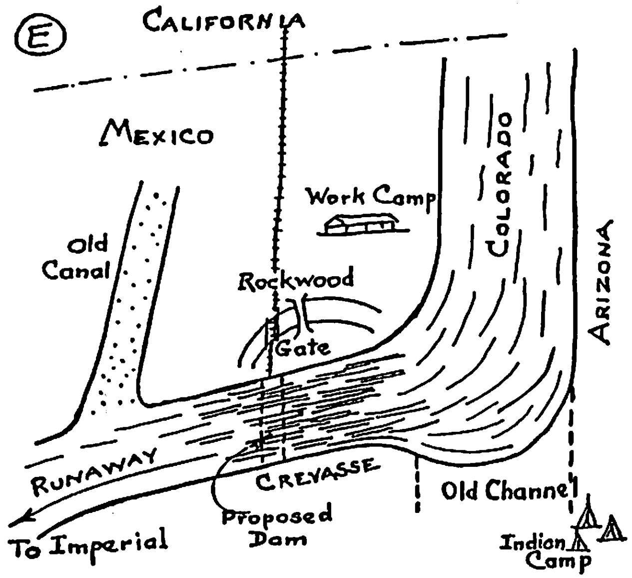

Cory's problem, August, 1906

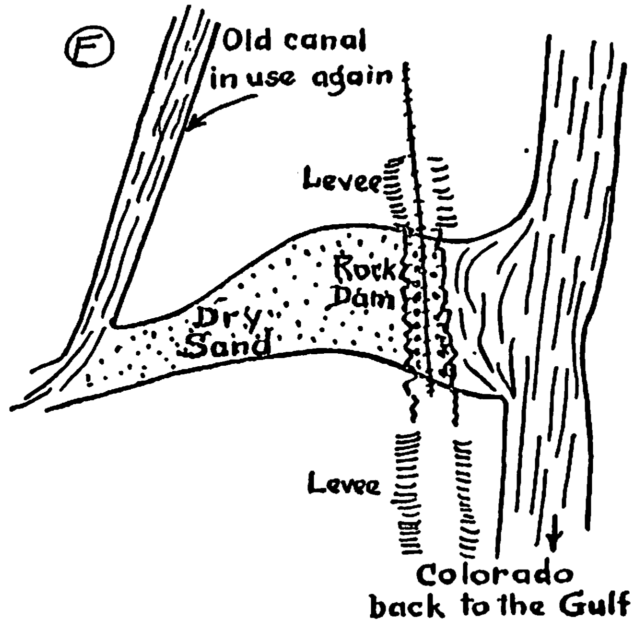

Cory's first victory, November, 1906

southeast of the clay occurrence at the Skeleton Canyon mine have a moderate potential for clay resources, although undiscovered clay resources are unlikely to be economic. The area southwest of the San Andreas fault has low potential for oil and gas resources and the entire study area has moderate potential for low-temperature (less than 90 °C) geothermal resources. The study area has low potential for barite and strontium resources.

INTRODUCTION

This mineral survey was requested by the U.S. Bureau of Land Management and is a joint effort by the U.S. Geological Survey (USGS) and the U.S. Bureau of Mines (USBM). An introduction to the wilderness review process, mineral survey methods, and agency responsibilities was provided by Beikman and others (1983). The U.S. Bureau of Mines

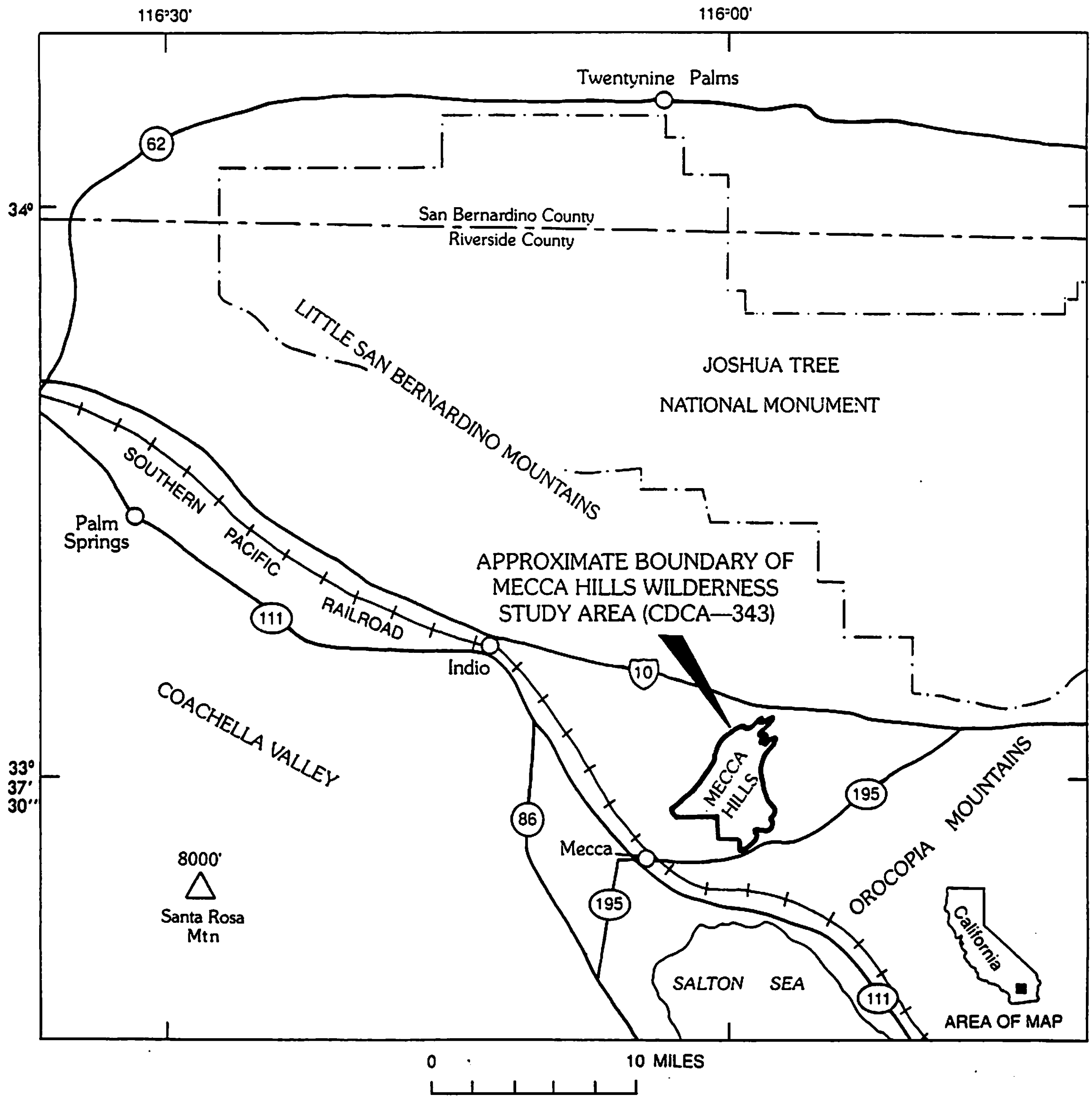

Figure 1. Index map showing the location of the Mecca Hills Wilderness Study Area, Riverside County, California.

J. Pedicino , from U S Geological Survey Bulletin 1710-C

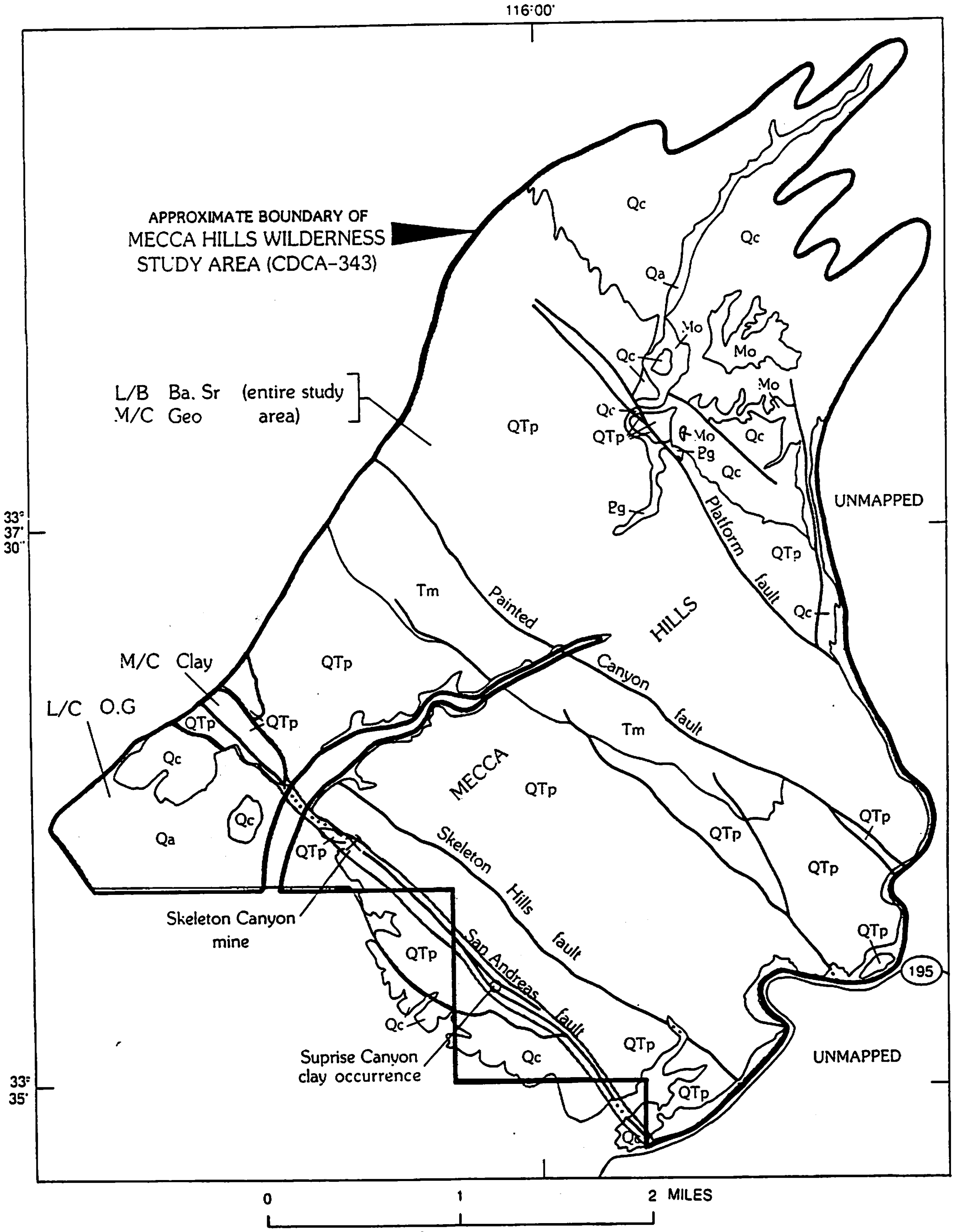

Figure 2. Mineral resource potential and generalized geology of the Mecca Hills Wilderness Study Area, Riverside County, California. Geology from A.G. Sylvester (unpub. data, 1985).

J. Pedicmis, from US Geological Survey Bulletin 1710-C.

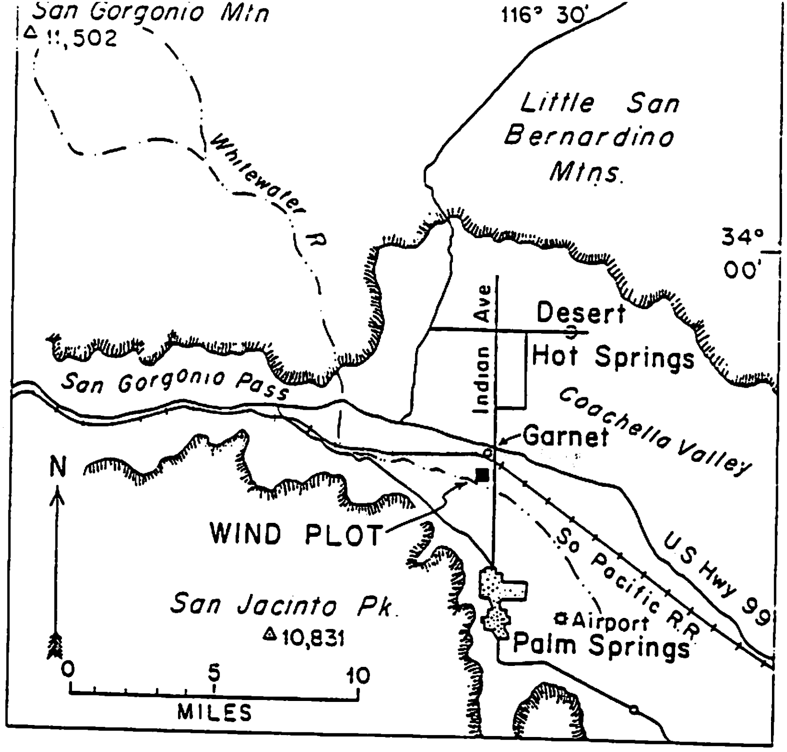

FIGURE 2-1. Location map of Garnet and aeolian erosion study area (from Sharp, 1964).

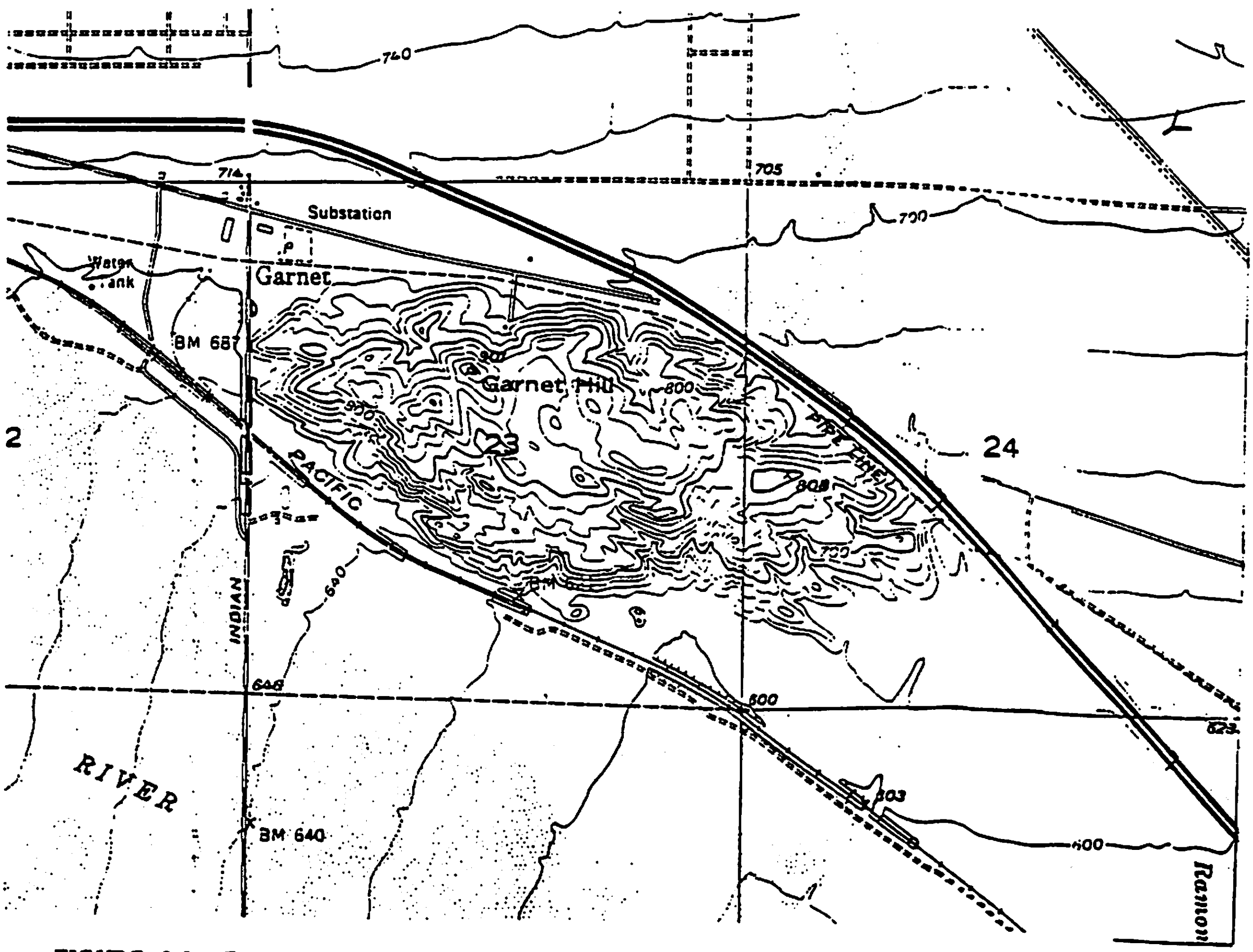

FIGURE 2-2. Enlargement of U. S. Geological Survey

Fig. 4.14. Map of Garnet Hill, showing the orientation of ventifact surface features which, taken together, show the wind flow over the hill. (From Hunter, 1979.)

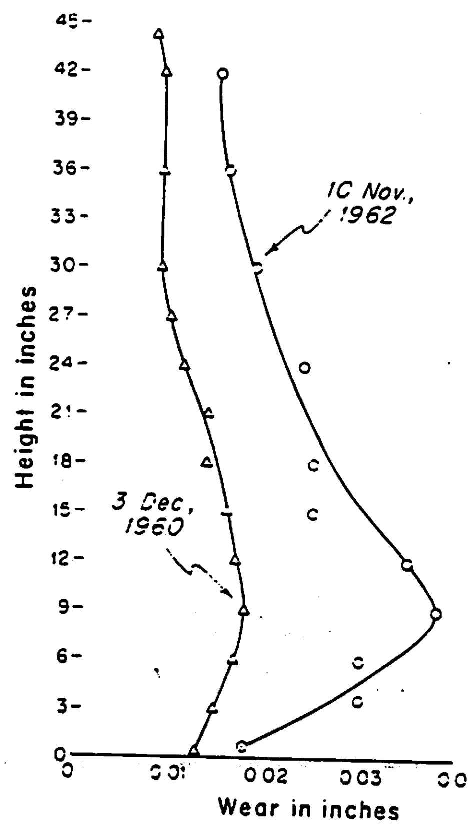

FIGURE 2-4. Wear by sand blast on a lucite rod anchored in the experimental plot (from Sharp, 1964).

NOLAN 30

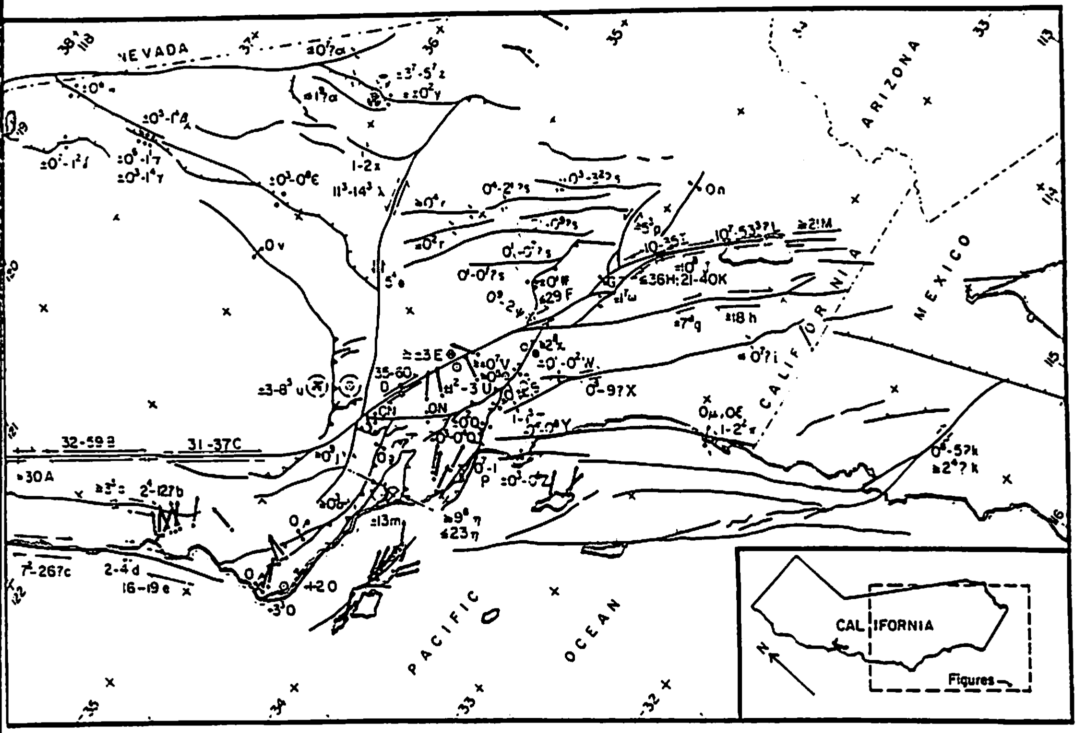

Figure 2. Mapped traces of active faults in the southern California area (inset) and their rates of slip. Fault traces, dips, and directions of motion from Jennings (1975) and others cited in text. Rates are in mm/yr, with tenths of mm/yr as superscripts. Prefix ≤ indicates an upper limit, ≥ indicates a lower limit, ± indicates relative vertical motion, and ~ indicates absolute uplift of one side. Horizontal arrows and vertical arrowheads (circles) have sizes proportional to rate of that component of slip wherever possible. Connected dots indicate no motion. Letters following numbers are keys to references in Table 1. Heavy, single arrows are paleomagnetic declinations of Neogene rocks (from Luyendyk and others, 1980).

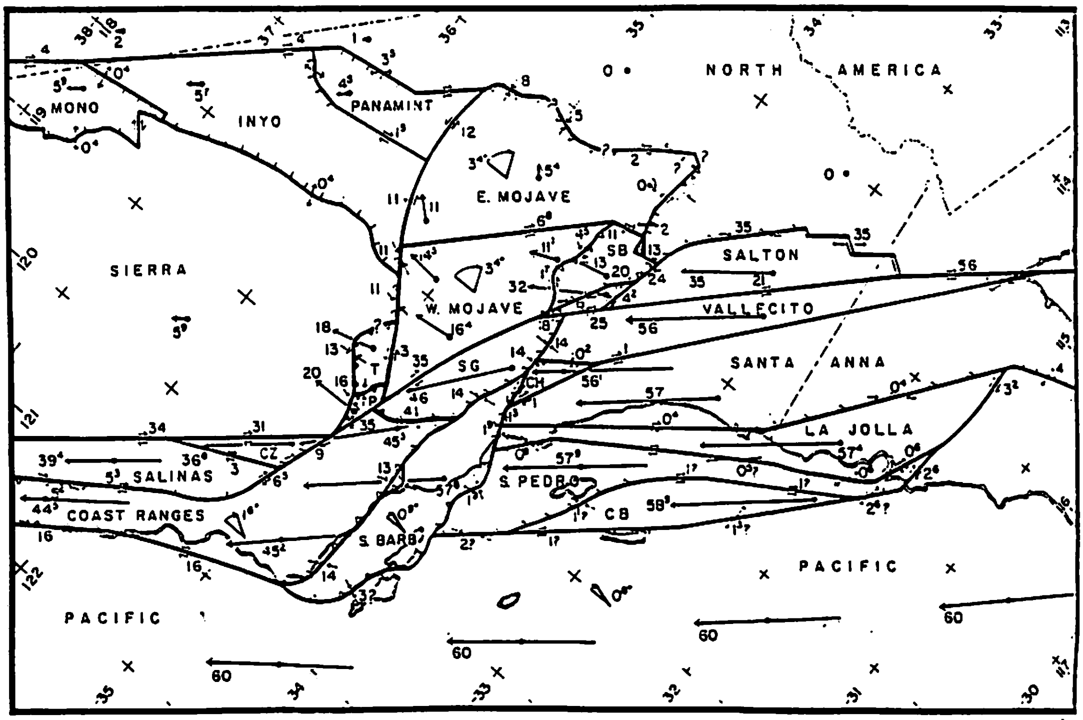

Figure 3. A proposed block model that satisfies most of the data from Figure 2. Heavy lines are block-bounding faults, triangular teeth show dip of thrusts, and straight ticks show dip of normal faults. Arrows from or through heavy dots show velocity with respect to North America at that point and are labeled in mm/yr. Double arrows along boundaries show sense and direction of relative block motions but are not proportional in size to the rate indicated. Arcs show a hypothetical change in declination produced by multiplying current rotation rates (given in degrees/m.y.) by 20 m.y. For further detail, consult Table A. Abbreviated block names: CB = Catalina Basin, CH = Chino, CZ = Carrizo Plain, P = Pleito Hills, R = Redlands, SB = San Bernardino Mountains, SG = San Gabriel Mountains, T = Tehachapi Mountains.

Transverse Ranges vs. the San Andreas Fault

Scenario 1: Extension in northern part of Basin and Range creates the Big Bend in the San Andreas Fault, leaving a thrust zone where the strike slip fault is split.

Scenario 2: The San Andreas was split because of natural weak slip joints: it's easier to maintain the thrust zone than to make a new slip joint.

Data that suggest that the blocks that make up the transverse ranges are rotating clockwise. this suggests that the fault is straightning out. This in turn suggests that either (2) is right, or that the extension in (1) is no longer behaving the same as when the Big Bend formed.

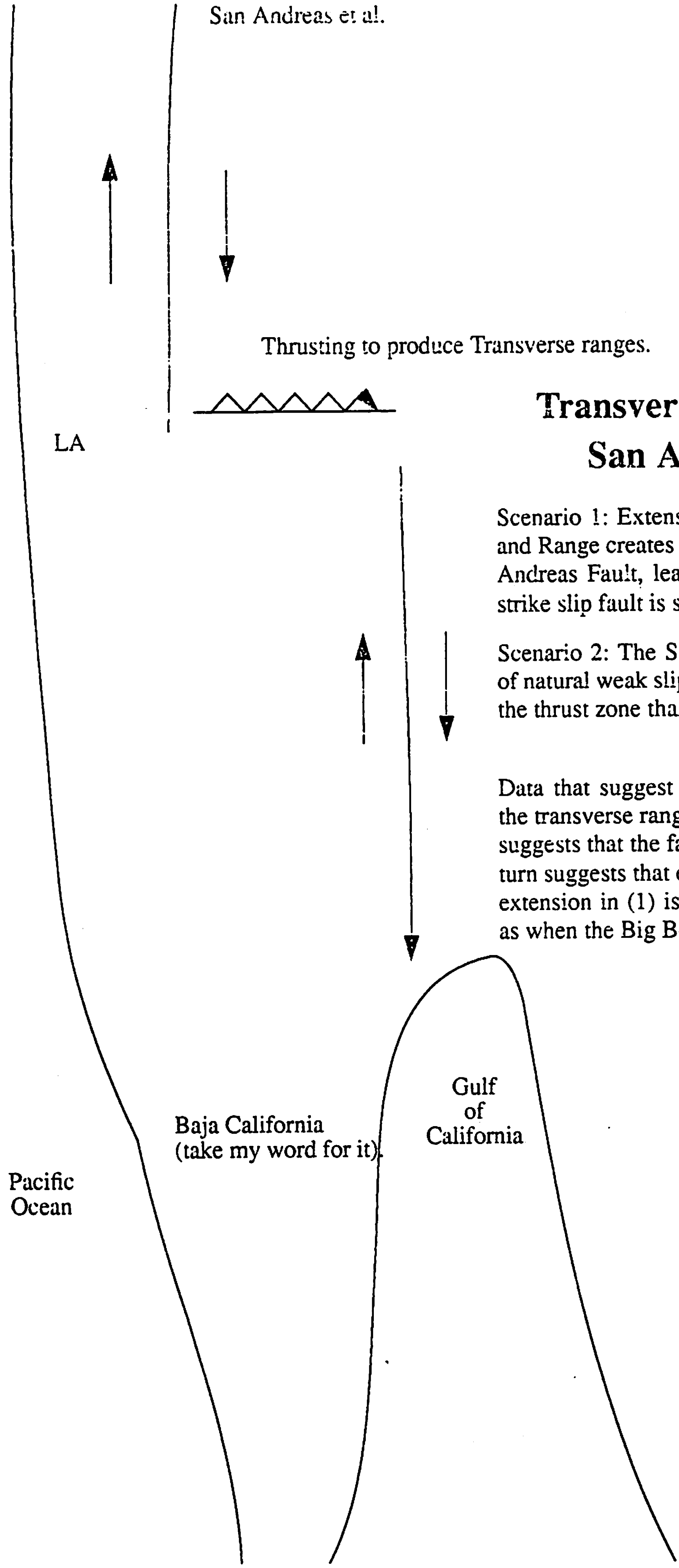

Geology of Blackhawk Canyon region/San Bernadino Mts

Jeff Johnson, PTYS 594a

STRATIGRAPHY

■ *Pre-Pliocene Rocks*:

1) Basement rocks are Precambrian (?) **biotite gneiss** intruded by light-gray, coarse-grained **biotite quartz monzonite.**

2) Carboniferous **Furnace Limestone** is coarsely crystalline, medium-gray marble; almost all of landslide lobe is composed of this marble.

3) Jurassic/Cretaceous (~155 My?) **Cactus Granite** is composed of light-gray **quartz monzonite** (*qtz-plag-orthcl-biot*; intrudes the Furnace Limestone) and dark-gray/black **quartz diorite** (*plag-hbl-biot-qtz*; intrudes Furnace LS and is intruded by the qtz. monz.)

■ *Pliocene Rocks*:

1) **Old Woman Sandstone:** Poorly-to-slightly sorted alluvial fan deposit of massive, reddish conglomeritic arkose and yellowish, relatively unbedded siltstones exposed on lower slopes of canyon with some volcanic clasts from sources to the north.

2) **Cushenbury Springs formation:** Series (seven-members) of fanglomerate/landslide breccias derived from Furnace LS, mostly covered by alluvium. *Member 4* is the Silver Reef breccia (3 miles long x 2 miles wide, east of Blackhawk), identical to the Blackhawk (*Member 7*) except that it is completely cemented. *Member 1* underlies *Member 7*, implying that it has been carried some 4 miles north by the landslide.

STRUCTURAL HISTORY

■ *Miocene/middle Pliocene*:

South-directed thrusting uplifted central and western portions of ancestral San Bernadinos, forming the extensive alluvial apron that became the Old Woman SS.

■ *Middle Pliocene/Quaternary*:

Early to middle Pliocene saw uplift of a broad north-central plateau, forming "North Frontal Thrust" area, south-southwest of Blackhawk Canyon, with predominantly northward motion. This causes a drastic change from the alluvial/fluvial environment of the Old Woman SS to the fanglomerates of the Cushenbury Springs Fm. (at about 2.0-3.2 Ma), both of which are overridden by these range-front thrusts.

A model proposed by [3] suggests that the northern plateau of the San Bernadinos was uplifted by northward motion along a deep crustal detachment ramp which coincides with the south-dipping plane defined by seismic studies. This would move the mountains as an entire block, which helps to explain the relative lack of deformation in the interior of the plateau. The 10% dip of this plateau suggests about 6 km of northward motion along this proposed ramp; but only about 3km of displacement is thought to have occurred along the front-range thrusts--the remainder might be explained by the ramp flattening near the surface, leading to motion along a subhorizontal surface with the Mojave Desert block itself.

Monoclinal warps are associated with this thrusting; the north-northwest trending Blackhawk monocline occurs at the mouth of Blackhawk canyon, folding the Old Woman SS and *Member 1* of the Cushenbury Springs Fm. Locations where these thrusts have been warped by monocline formation so that they dip parallel to the range front slope are prime sites for landslides.

REFERENCES: [1] Shreve, R.L., 1968, GSA Spec. Paper 108, 47p.
[2] Shreve, R.L., 1987, GSA Centennial Field Guide--Cordilleran Section, p. 109.
[3] Meisling, K.E., and Weldon, R.J., 1989, GSA Bull., **101**, p. 106.

Johnson / Grandy

33

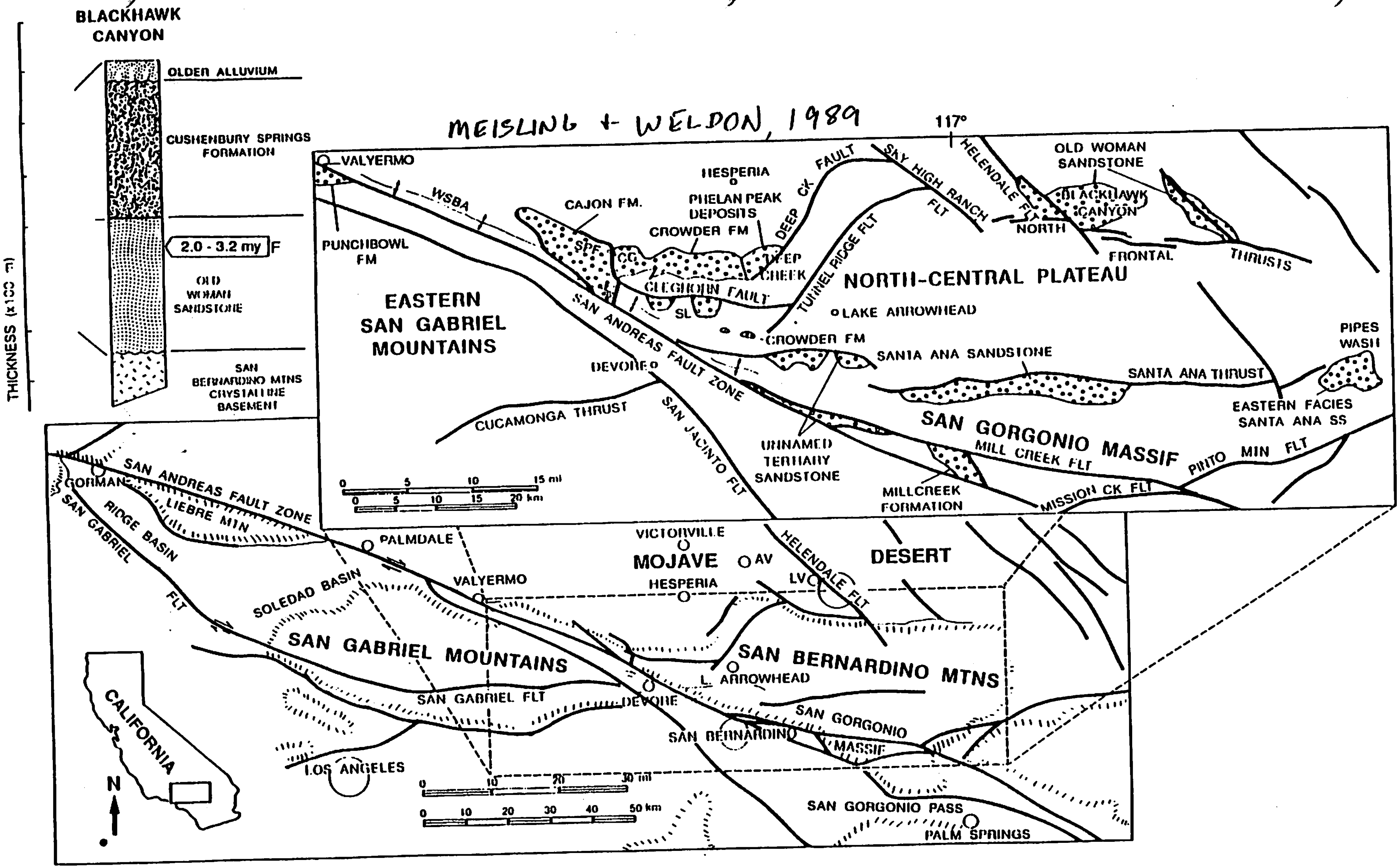

Figure 1. Index map of the San Bernardino Mountains and their relationship to the central Transverse Ranges in southern California, showing the location of major physiographic and cultural features, as well as principal regional faults and exposures of late Cenozoic sedimentary rocks (open circle pattern). See Figure 2 for geologic map of study area. Line of seismicity cross section of Figure 9 is longitude 117°W. LV: Lucerne Valley; AV: Apple Valley; WSBA: Western San Bernardino arch; CC: Crowder Canyon; SL: Silverwood Lake; SPF: Squaw Peak fault.

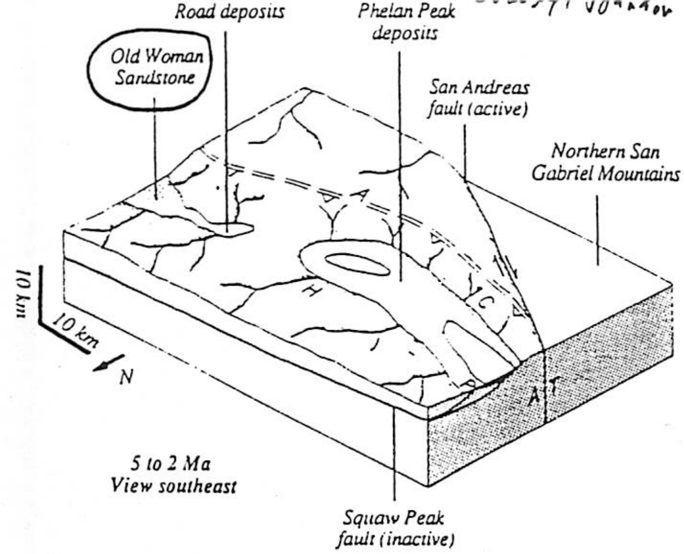

Figure 12. Paleotectonic block diagram of the study area during development of the Phelan Peak basin in Pliocene time (5 to 2 Ma). A marked change in depositional patterns throughout the western San Bernardino Mountains is reflected in the rocks of the Phelan Peak deposits, Old Woman Sandstone, and Santa Ana Sandstone. Deposition appears to have been confined to a narrow east-west- to northwest-southeast-trending trough. Strata deposited in the Pliocene trough are characterized by distinctive fine-grained volcanogenic and lacustrine sequences with rapid facies and/or thickness variations. The existence of a region of uplift confining the trough on the south is supported by the occurrence of clasts of local affinity in the Phelan Peak deposits and Old Woman Sandstone. Uplift may have been an early expression of north-directed thrusting, or residual relief related to the Squaw Peak thrust system. The San Andreas fault was active at the western edge of the study area at this time. A: Arrowhead; C: Cajon; H: Hesperia; P: Phelan.

Figure 13. Paleotectonic block diagram of the study area during deformation and uplift associated with development of the North Frontal thrust system in early Pleistocene time (2.0 to 1.5 Ma). Most of the relief on the prominent north frontal escarpment of the San Bernardino Mountains developed by thrusting and warping during this time. North-directed thrusts overrode the Old Woman Sandstone and uplifted the broad central plateau of the San Bernardino Mountains. Early to middle Pleistocene uplift of the plateau without disruption of internal drainage is modeled by northward movement of the San Bernardino Mountains block up a detachment ramp at a depth of 5–12 km beneath the range. We interpret range-front warping as a geometric consequence of northward shallowing of the deep-seated master thrust system where it merges with the detachment horizon beneath the Mojave Desert. The Ord Mountains frontal faults and Tunnel Ridge fault are the surface expression of a lateral ramp in the detachment surface. West of these structures, deformation appears to have been taken up by predominantly left-lateral motion on the Cleghorn fault. A: Arrowhead; C: Cajon; H: Hesperia; P: Phelan.

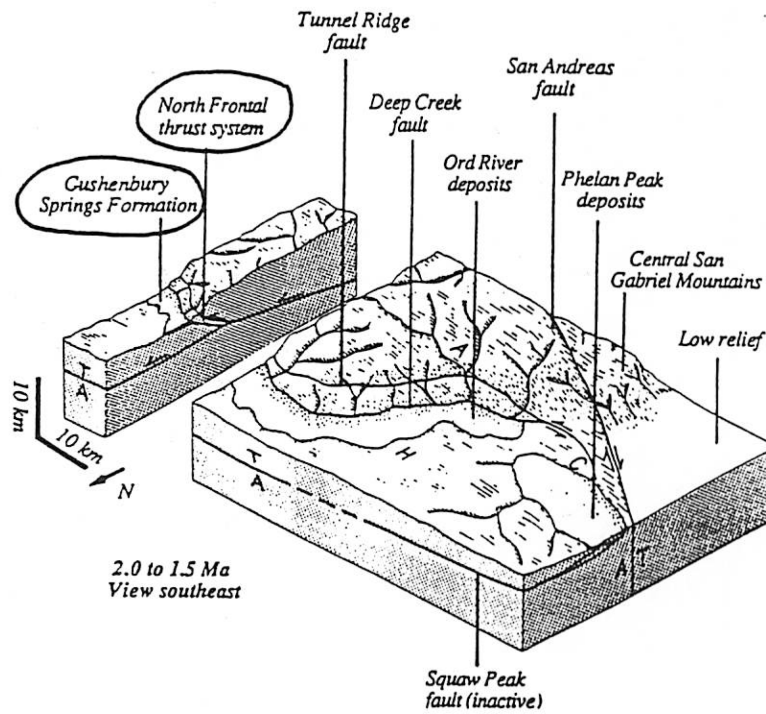

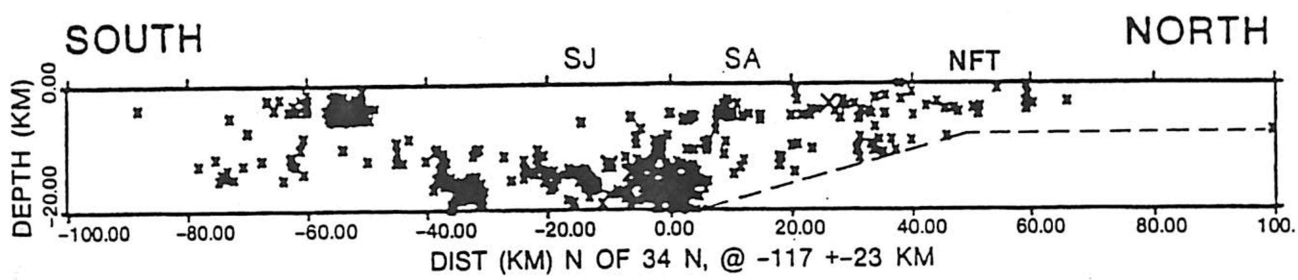

Figure 9. Microseismicity beneath the central San Bernardino Mountains. Cross section shows depth of seismic events of quality A from October 1981 to August 1983 projected to longitude 117° (the center line of the northern-central plateau; see Fig. 1) from the region between 116°45′ and 117°15′. SA and SJ indicate the location of the San Andreas and San Jacinto faults, respectively. NFT indicates the location of the North Frontal thrust system. Seismic events do not occur below a "floor" (dashed line) which rises from about 12 km beneath San Gorgonio Pass to less than 5 km beneath the Mojave Desert. Our proposed early Pleistocene detachment ramp coincides with the seismicity "floor," which is interpreted to reflect a contrast in mechanical behavior or decoupling in the upper crust. The seismicity ramp would project to the surface 20 to 30 km north of the north frontal thrusts; we postulate that it actually flattens and merges with a horizontal detachment plane at about 5 km beneath the Mojave block (figure adapted from Corbett, 1984).

Johnson / Grundy

Comparison: Blackhawk and El Capitan Landslide Statistics

	Blackhawk	El Capitan
Volume of rock involved	3×10^8 m^3	4×10^7 m^3
Maximum vertical drop	1.2 km	1.3 km
Maximum horizontal travel	9 km	6.8 km
Deposit thickness	10 - 30 m	5 - 35 m
Maximum deposit width	3 km	1.5 km
Age of landslide	17400±550 bp	Pleistocene (?)
Rock type in landslide	Furnace limestone, (actually a dolomitic marble)	Devonian and Mississippian limestone
Substrate material	fanglomerate and sandstone	conglomerate and playa
Modal fragment size	2.5 cm	?
Estimated landslide velocity	35 m s^{-1}	?

Things to look for:

Look for preservation of original stratigraphy.

sliding

gliding (like a hovercraft)

ballistic

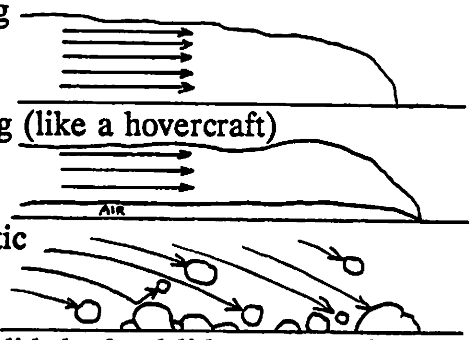

What sort of transport happened here?

turbulent flow

power-law flow

laminar flow

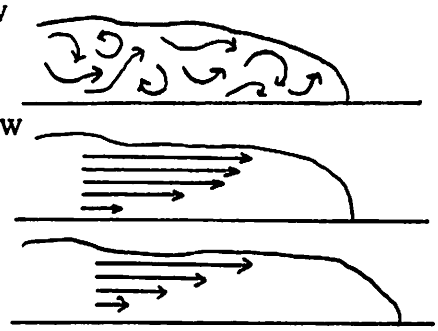

How did the landslide stop moving? Abruptly or gradually? Front or rear first? Look for bulldozed substrate material, imbrication of landslide toe, clastic dikes.

What kind of environment did rocks experience inside of the avalanche? Compare them with the shocked rocks we saw at the Nevada Test Site. Look for evidence of fracturing, melting, or vaporization. Look for slip surfaces, slickenslides.

In the breccia, what is the ratio of matrix to rock? How variable it that ratio?

Some Hypotheses Explaining the Mobility of Large Rock Avalanches

Air trapped by debris fluidizes avalanche by rushing out through debris and supporting part of its weight.

Avalanche traps air under itself at sufficient pressure to balance acceleration of gravity, so debris flies like a hovercraft.

Water or dust fluidizes avalanche debris via buoyancy.

Avalanche debris acts like energetic gas of particles in which energy and momentum are transferred via collisions.

Intense friction melts or vaporizes rocks locally, providing lubrication where most needed.

Water vapor given off by debris fluidizes avalanche debris.

Acoustic waves from crunching, grinding rocks at base of avalanche have sufficient amplitude to relieve local stresses.

Earthquakes trigger big avalanches and fluidize them via low frequency seismic waves.

Motion along substrate produces sufficient shear at base of avalanche to dilate debris so Bagnold grain flow can occur.

"Avalanche" deposit actually hand-emplaced by LPL grad students after dark, March 31.

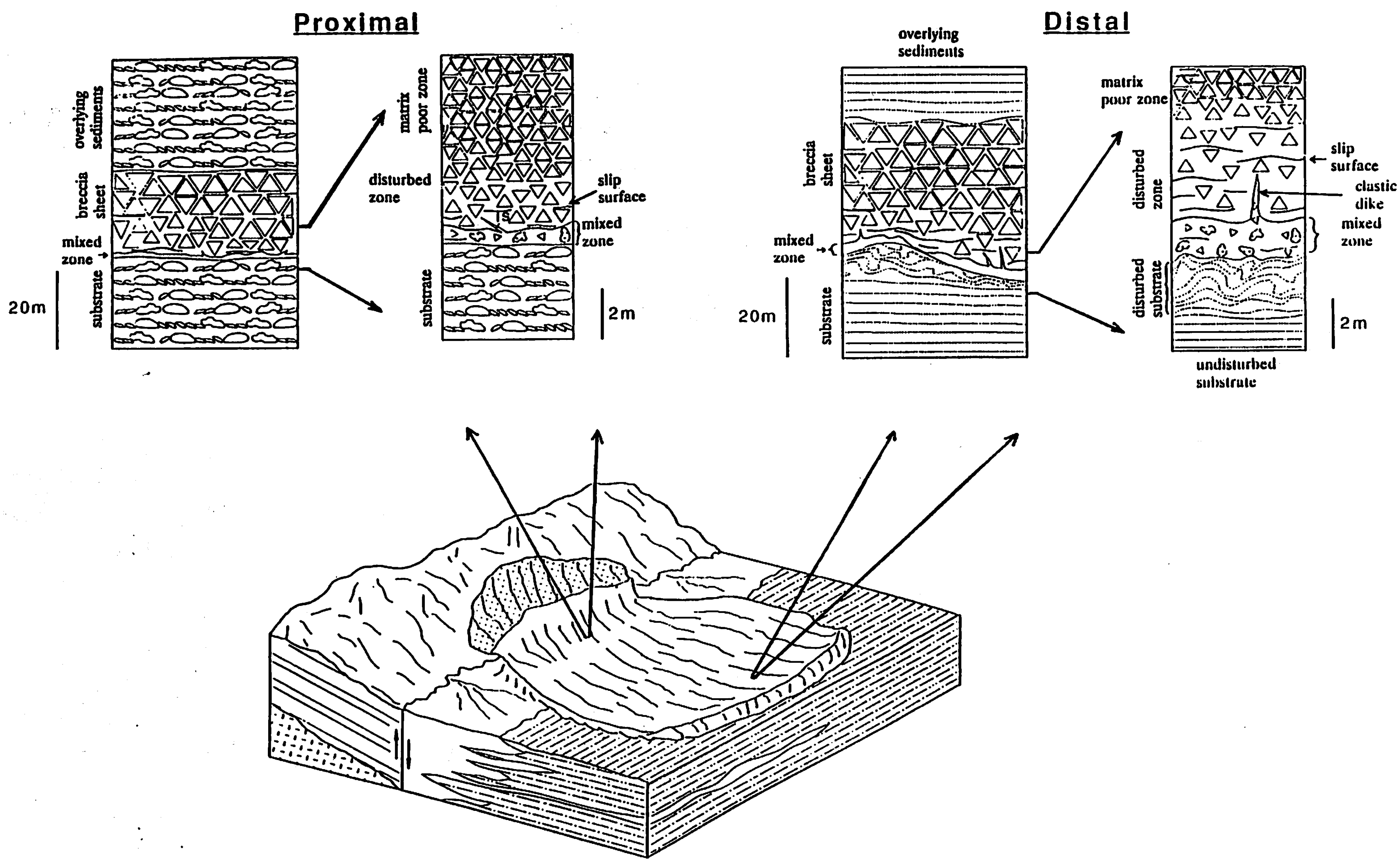

Morphology of a Large, Dry Rock Avalanche Deposit

Johnson / Grundy

Grundy / Johnson

38

Yucca Valley →

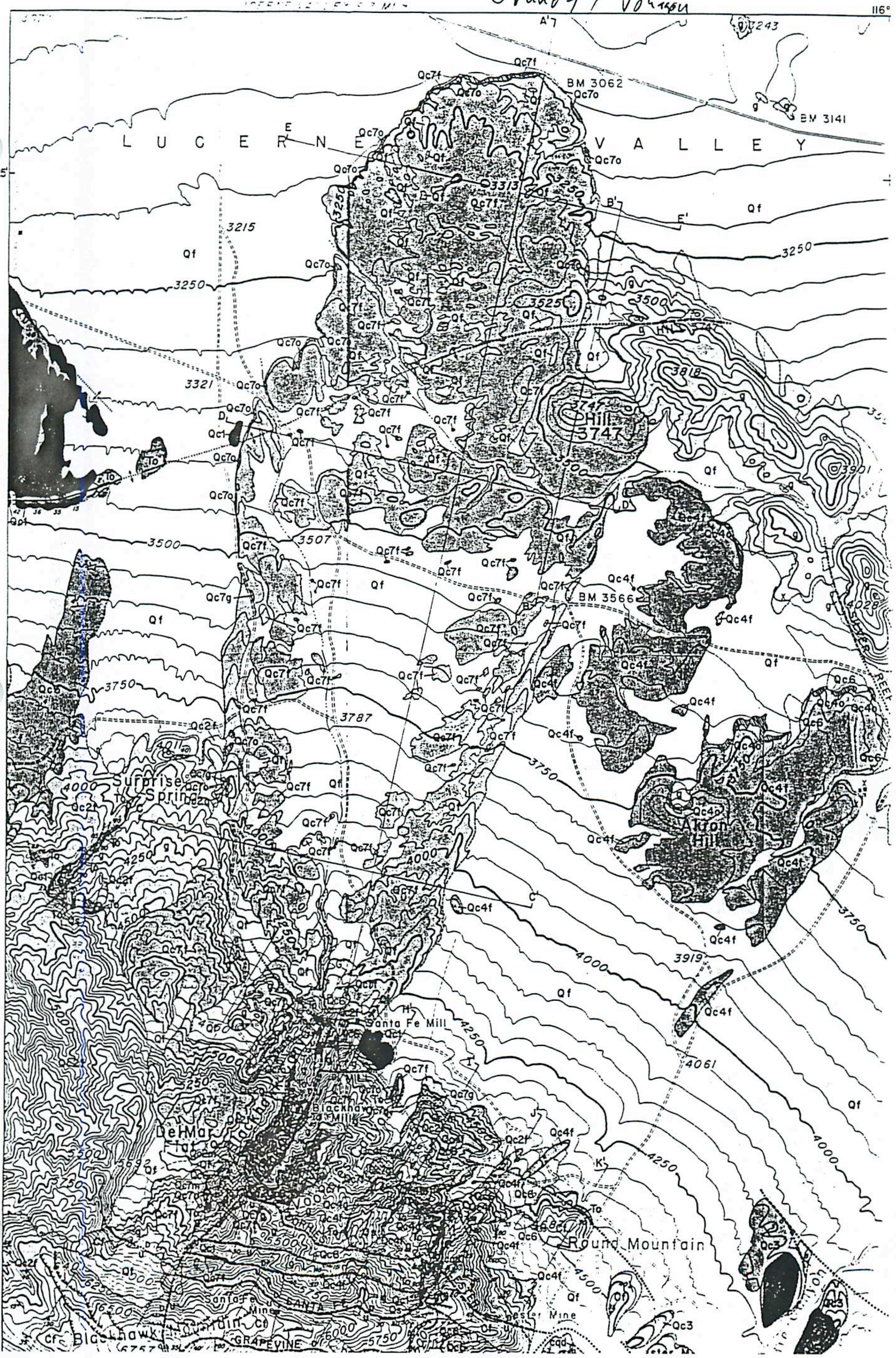

Johnson / Grundy

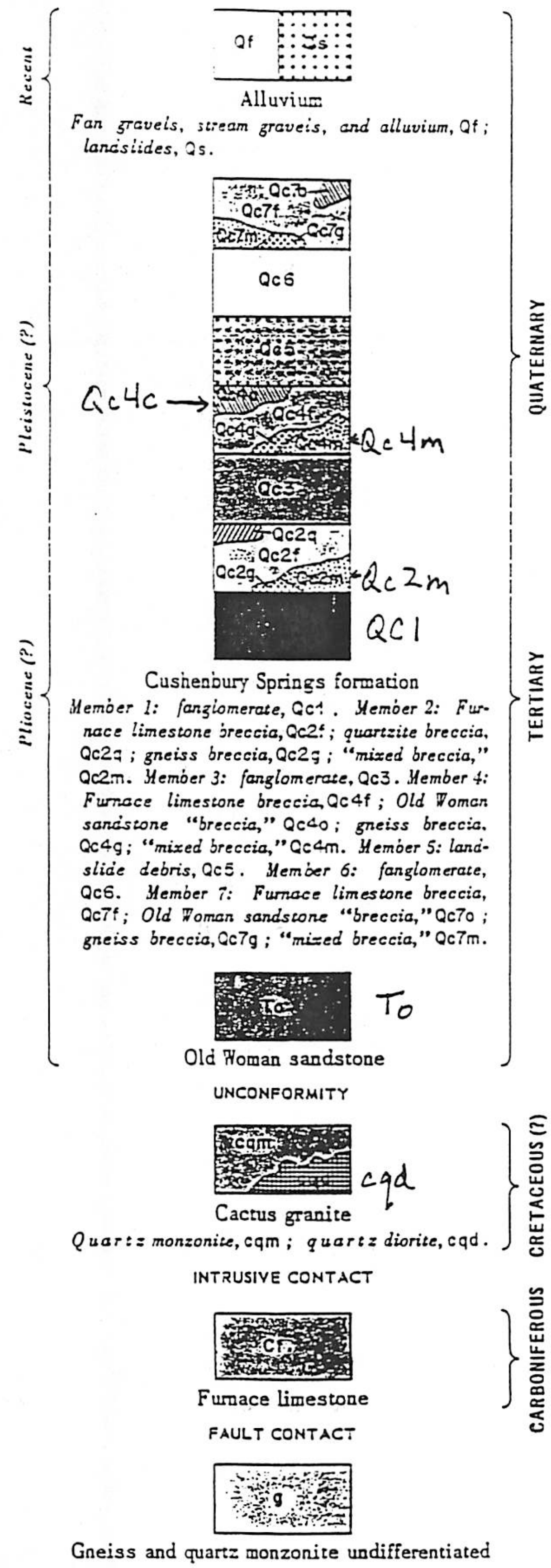

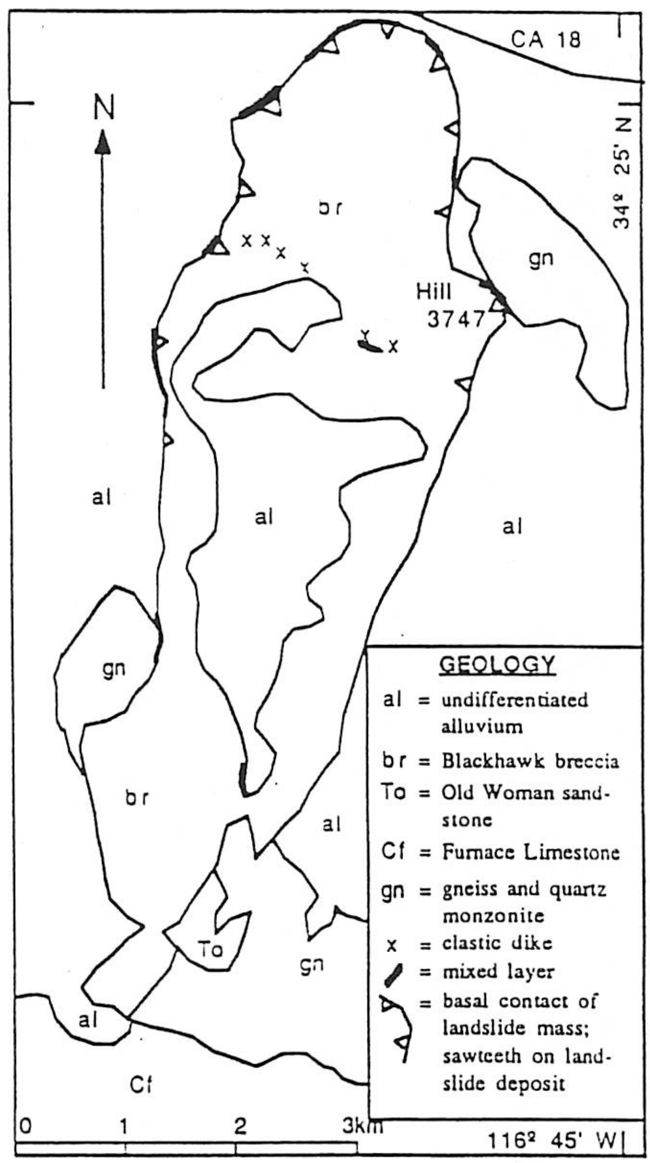

Figure 14. Simplified geologic map of the Blackhawk breccia in San Bernardino County, California. Modified from Shreve (1968, 1987) and Johnson (1978).

Pierazzo / Herron

40

Geology of the Joshua Tree Monument

Joshua Tree National Monument is a 557,000 acre area set aside to preserve a piece of typical California desert.

The Monument region is made up of several distinct mountain ranges, the **Little San Bernardino Mountains** in the southwestern part, the Cottonwood, **Hexie**, and **Pinto Mountains** in the center, and the **Eagle** and Coxcomb Mountains in the eastern part. Much of the Monument lies at elevations above 4,000 ft.

Valleys lying between these mountain ranges are of two types, those that have been formed by downdropping along faults (grabens or structural basin), like **Pleasant Valley**, and those that have been carved by erosion. like **Queen Valley**.

Uplifting and downdropping, and horizontal slipping of crustal blocks in the Joshua Tree regions has occurred along faults. The most prominent faults in the region, both leftlateral, are the Pinto Mountain fault, extending almost east–west along the north side of the Pinto Mountain, and the Blue Cut fault extending east–west through the Little San Bernardino Mountains, under Pleasant Valley, and into the Pinto Basin. In addition to the major faults are many hundreds of minor faults throughout the region. Fault zones are important in localizing springs. The oasis at **Cottonwood Springs**, for example, appears to be due to a fault zone which has provided the fissures along which ground water reaches the surface.

One of the most impressive aspects of the landforms in the Joshua Tree region is the strange and picturesque shapes assumed by the bold granitic rock masses like in the Split Rock area. This is the result of the combined action of rock jointing, chemical and mechanical weathering, and erosion. The joint system in the White Tank monzogranite consists of three dominant joint sets. One set oriented horizontally has been caused by the release of pressure due to the removal of overlying rocks by erosion. These joints cause rock sheeting. The other two sets of joints are oriented vertically and perpendicularly to each other. The resulting system of joints froms rectangular blocks. like at **Jumbo Rocks**, and **Split Rock**. Chemical or spheroidal weathering results from slight pressures that have been built up in the outer portion of the rock from chemical decomposition of. mainly, the aluminum silicate minerals, along joint surfaces.

For example, when potassium feldspar ($KAlSi_3O_8$) comes into contact with H^+ and H_2O, the following chemical reaction takes place:

$$2KAlSi_3O_8 + 2H^+ + H_2O \rightarrow Al_2Si_2O_5(OH)_4 + 2K^+ + 4SiO_2$$

The potassium ions and silica are dissolved in water and eventually carried away, leaving behind the kaolinite (clay) that occupies a greater volume than the original feldspar, causing the cuboidal block of rock to expand. Frost and root wedging contribute to the breakdown of rocks by mechanical action.

Weathering and erosional processes presently operating in the arid conditions of the Joshua Tree region cannot be entirely responsible for the spectacular sculpturing of the rocks of the region. The present Joshua Tree landscape, and that of much of the Mojave Desert, is essentially a collection of relict features inherited from earlier times of higher rainfall and lower temperatures.

Among the typical arid landforms of the high deserts, **pediments**, like the one at **Malapai Hill**, are common of deserts of the southwestern United States. Pediments are erosional features on gently sloping bedrock surfaces that have been carved along the base of desert mountains. Superficially they look like bajadas (broad sloping aprons of sediment that result from the coaliscing of many alluvional fans) rather than products of erosion of bedrock. The slopes of pediments vary between 0.5° to about 6° and they are usually carved on homogeneous crystalline rock such as granite.

The origin of pediments may be closely linked to the origin of inselbergs, prominent steep–sided residual hills and mountains rising abruptly from erosional plains (fig.1). Climatic conditions during the late Tertiary and the Pleistocene must have been significant in the development of pediments and inselbergs.

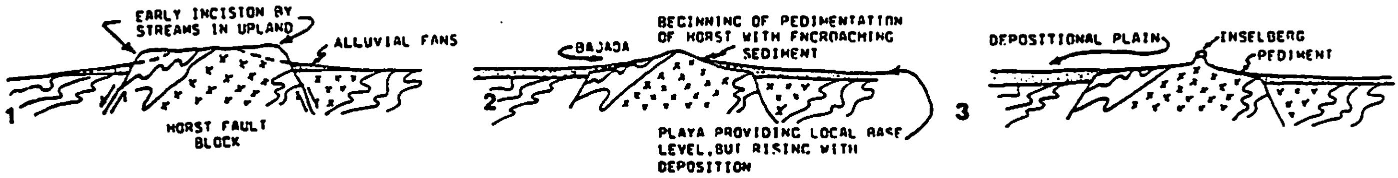

Figure 1: Pediment and inselberg development in the southwestern United States from a combination of deep weathering of a horst upland, stream erosion, and rising base level in the adjacent down–faulted basins (after Garner, 1974, and Bradshaw and others, 1978).

Rock types of Joshua Tree National Monument

Metamorphic Rocks. The oldest rocks of the Joshua Tree region are those of the Precambrian Pinto Gneiss which range in composition from quartz monzonite to quartz diorite. Much of the rock is dark-gray and prominently foliated, but some is much lighter, sometimes nearly white white and only faintly foliated. The gneiss is composed primarily of quartz, feldspar, and biotite. Where there is a significant amount of biotite the Pinto Gneiss is very dark and this distinguishes it from the other rocks in the area.

The Pinto Gneiss, formed from the metamorphism of pre-existing sedimentary and igneous rocks. Radiometric dates give two ages of metamorphism, 1650 million years and 1400 million years. These rocks make up the core of the Little San Bernardino, Pinto, Hexie, Eagle and Coxcomb Mountains. They are easily seen at Salton View (Keys View), along the road through Berdoo Canyon and on the trail to the summit of Ryan Mountain.

Igneous Rocks. The Pinto Gneiss served as the host rock into which younger plutonic rocks intruded. At least four different major plutons have intruded the Pinto Gneiss. The Mesozoic Plutons in Joshua Tree National Monument are believed to have originated in an Andean-type tectonic environment. The exact ages of these intrusion is uncertain. The Jurassic plutons are the oldest and fall generally between 186 and 156 million years; the Cretaceous plutons are the youngest and are mainly between 155 and 126 million years.

- **Twentynine Palms Porphyritic Quartz Monzonite.** The oldest pluton is of the Jurassic plutonic belt and is the Twentynine Palms Porphyritic Quartz monzonite. It consists of a matrix of small mineral grains which enclose large phenocrysts of potassium feldspar crystals that attain lengths of up to two inches. The rock crops out at the beginning of the trail to Fortynine Palms Oasis and is exposed along the arroyo on the east side of the Indian Cove campground.
- **Queen Mountain Monzogranite.** The oldest of the Cretaceous plutons is the Queen Mountain monzogranite which is exposed over a large area around Queen Mountain. It is coarse-grained, and consists of plagioclase, potassium feldspar, quartz, and either biotite or biotite and hornblende.
- **White Tank Monzogranite.** The light-colored, Cretaceous White Tank monzogranite resembles the Queen Mountain monzogranite but differs by being finer-grained, and by containing very small amounts of biotite and/or muscovite but no hornblende. Areas underlain by the White Tank Monzogranite include Indian Cove, The Wonderland of Rocks, Jumbo Rocks, White Tank and Lost Horse Valley.
- **Oasis Monzogranite.** The youngest of the Cretaceous plutons, the Oasis monzogranite, is a distinctive garnet- muscovite-bearing pluton that is exposed in the area of Fortynine Palms Oasis. The garnets are blood red and small, but large enough to be visible without magnification. The muscovite grains impart a glittery appearance to the rock on sunny days, even in shadows.
- **Other Plutons.** In addition to large monzogranite and quartz monzonite plutons, there are masses of a similar granitic rock called granodiorite. and small dark plutons called Gold Park diorite.
- **Dikes.** Cutting across all of the aforementioned rock masses and thus being younger in age are dikes of felsite, aplite, pegmatite, andesite and diorite. The pegmatite dikes are mainly quartz and potassium feldspar and have a composition close to that of granite. However. the pegmatite mineral grains are often three or four inches long. Pegmatites may have large books of biotite and muscovite mica (isinglass).
- **Milky Quartz.** The quart is sometimes stained reddish brown from the weathering of pyrites or fools gold. Pyrite is a common mineral in quartz veins and is sometimes associated with gold or other valuable minerals. Chemical alteration of the pyrite produces reddish iron oxides that stain the rock and serve as a clue the gold, silver, copper and other metals may be present.
- **Basalt.** Basalt occurs at three places in the Monument: (1) near Pinto Basin, where the basalt probably originated as extrusive flows; (2) at Malapai Hill on the Geology Tour Road (a volcano dome); and (3) in the Lost Horse Mountains.
- **Lherzolite.** Lherzolite occurs as inclusions within the basalt at Malapai Hill and in the Lost Horse Mountains. Lherzolite is approximately 75 percent olivine with the remainder consisting mostly of bronzite and diopside. It is considered to be derived from the mantle: thus the basalt has risen some 35 to 50 miles to carry lherzolite inclusions to the surface.

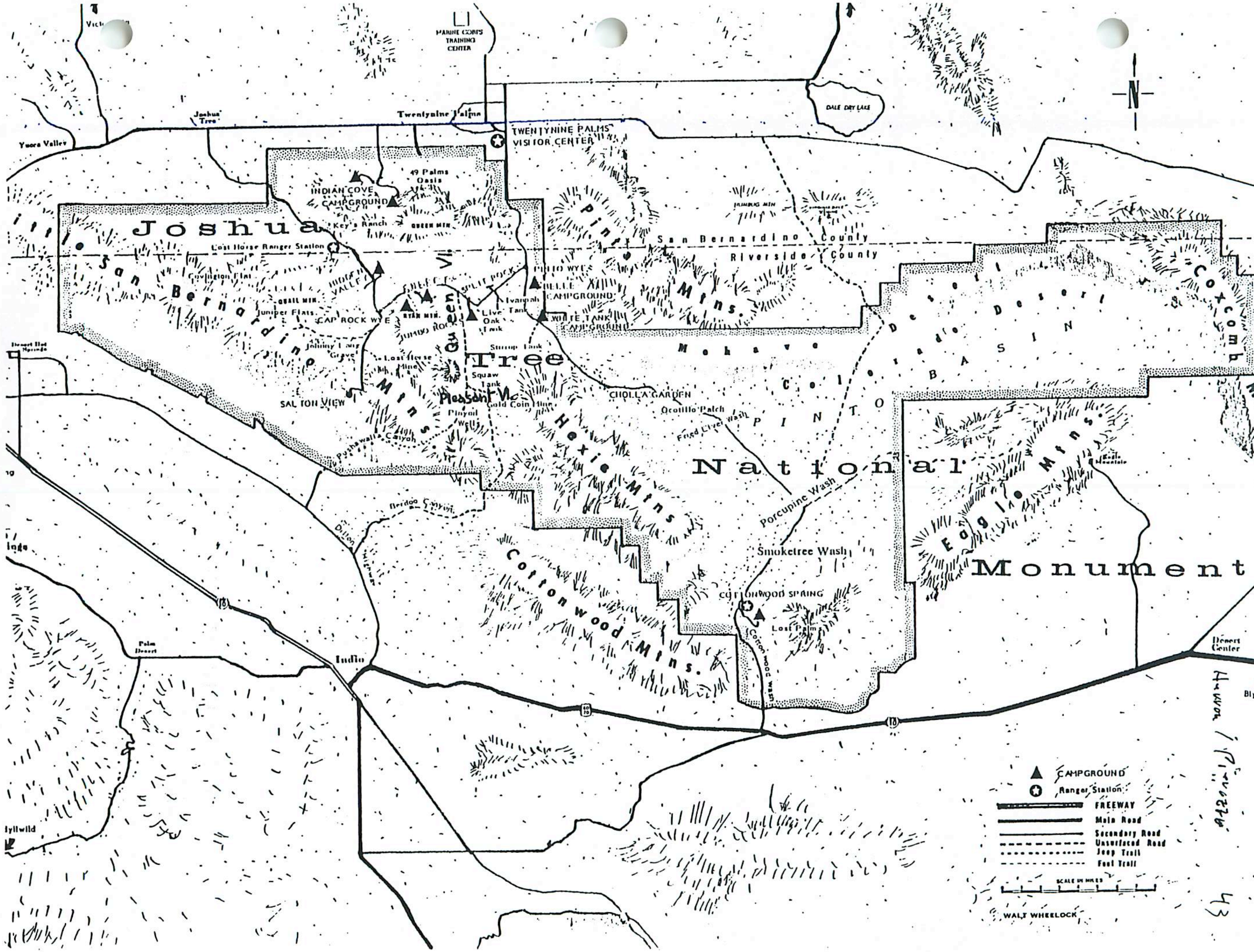

Joshua Tree National Monument
San Bernardino Mtns.
Pinto Mtns.
Hexie Mtns
Cottonwood Mtns.
Eagle Mtns.
Coxcomb
Little San Bernardino Mtns.
Queen Vly.
Pleasant Vly.
Mohave Desert
Colorado Desert
PINTO BASIN
San Bernardino County
Riverside County
TWENTYNINE PALMS VISITOR CENTER
MARINE CORPS TRAINING CENTER
Twentynine Palms
Joshua Tree
Yucca Valley
DALE DRY LAKE
JUMBUG MTN
49 Palms Oasis
INDIAN COVE CAMPGROUND
Key's Ranch
QUEEN MTN
Lost Horse Ranger Station
Covington Flat
QUAIL MTN.
Juniper Flats
CAP ROCK WYE
JUMBO ROCKS
RYAN MTN.
Johnny Lang Grave
Lost Horse Mine
SALTON VIEW
Pushawalla Canyon
Pinyon Well
Gold Coin Mine
Squaw Tank
Live Oak Tank
Ivanpah Tank
PINTO WYE
BELLE CAMPGROUND
WHITE TANK CAMPGROUND
CHOLLA GARDEN
Ocotillo Patch
Fried Liver Wash
Porcupine Wash
Smoketree Wash
COTTONWOOD SPRING
Lost Palms
Cottonwood Wash
Berdoo Canyon
Dillon
Indio
Palm Desert
Idyllwild
Desert Center
CAMPGROUND
Ranger Station
FREEWAY
Main Road
Secondary Road
Unsurfaced Road
Jeep Trail
Foot Trail
SCALE IN MILES
WALT WHEELOCK
Hurron / Pirozzo
43

THE EVOLUTION OF THE SONORAN DESERT

by your xeriphytic hostess, Cathy Steffens

THE GEOGLYPHS are designs in desert pavement depicting people, plants, animals, and abstract shapes up to 300 feet long. Hundreds of these designs have been found along the Colorado and Gila Rivers; they are similar to even larger geoglyphs near Nazca, Peru. Some rock alignments may be as old as 12,000 years, but most of the giant pictures appear to have been made about 1000 years ago. Modern native peoples still use the geoglyphs in their ceremonies and legends. The BLM protects the geoglyphs and the native Yuman people periodically repair them.

An expansion of southwestern native people from 380 - 1400 A.D. is associated with a period of high precipitation; the sudden "disappearance" of these people is associated with a winter drought about 1400 A.D. Some people think the geoglyphs were made as desperate entreaties to the gods to bring back the rivers, lakes and wildlife that flourished in an earlier, wetter climate.

MODERN DESERT PLANT COMMUNITIES of cacti, leguminous trees and shrubs have been in the northern Sonoran Desert region for only the last 4000 years, with the arrival of organ pipe, ironwood and foothills palo verde from Mexico. Saguaros, blue palo verde and brittlebush arrived 8-10,000 years ago from refugia in Mexico where they lived during the glacial periods.

18,000 years ago, at the height of the Wisconsin glaciation, the Lower Colorado River Valley was the home of pinyon pine, shrub oaks, juniper, Joshua Trees, creostote, saltbush and white bursage. Today the area is dominated by a relict population of creosote bush and white bursage. Creosote bush migrated from South America during the Pleistocene and has spread through the Chihuahuan, Sonoran and Mohave deserts only in the last 17,000 years.

The Gila Monsters, scorpions, and snakes thought to be representative of the desert actually evolved in the tropical deciduous forest in Mexico and are at their northernmost limits here. They were living in this region during the Pleistocene, when the surrounding vegetation consisted of oak woodland.

THE ADAPTATIONS that enable plants to survive in the arid southwest (succulence, deciduous habit, waxy or fuzzy covering on leaves, small leaves, CAM and C4 photosynthesis) probably evolved in the Paleocene or Eocene, but the plants themselves did not become widespread until the interglacials of the Pleistocene, when large areas of land became increasingly hot and dry.

WHAT IS CAM PHOTOSYNTHESIS? All cacti, agaves, and many other desert plants such as ocotillo have evolved a nifty mechanism for conserving water. CAM stands for Crassulacean Acid Metabolism. Plants with CAM open their stomates at night, when temperatures are lower and humidity is higher, to absorb CO_2, which they then store in the form of an organic acid. During the day, the plants keep their stomates closed, and the waxy cuticle of most succulents makes the plants almost waterproof. High temperatures during the day converts the organic acid back to CO_2. (A plant in CAM mode will taste acid in early morning and bland in the afternoon. But don't try this at home, kids; most local succulents are poisonous.) CAM plants can also go into an "idling metabolism" during droughts; they recycle the CO_2 in their tissues, keep their stomates sealed, and after a rain can resume full growth in 24 to 48 hours.

DURING THE EOCENE, families of ocotillo, jojoba, agave, cacti, and grasses evolved, but were confined to arid pockets in dry tropic forest. The climate was generally warm and wet.

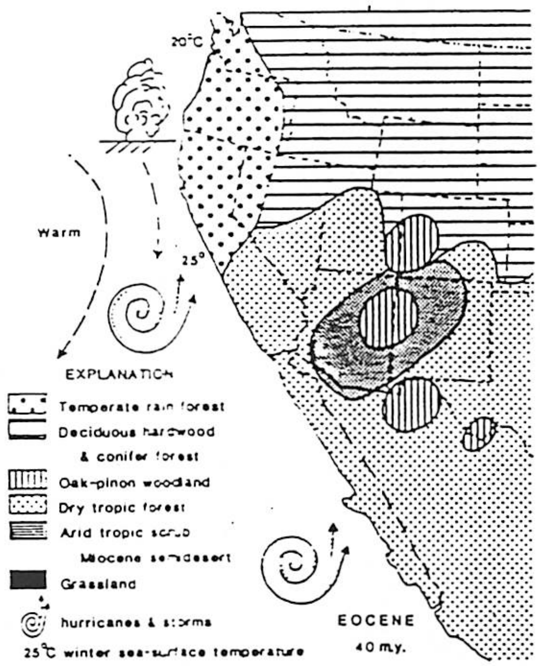

From Axelrod, 1979

DURING THE MIOCENE, the climate became cooler and drier with the uplift of the Rockies and Sierra Madres. Plants evolved several adaptations to seasonal dry periods:

- decrease in stature
- decrease in leaf size
- deciduous habit
- tough covering on leaves
- succulence
- CAM and C4 photosynthesis
- rapid flowering and seed production in wet season.

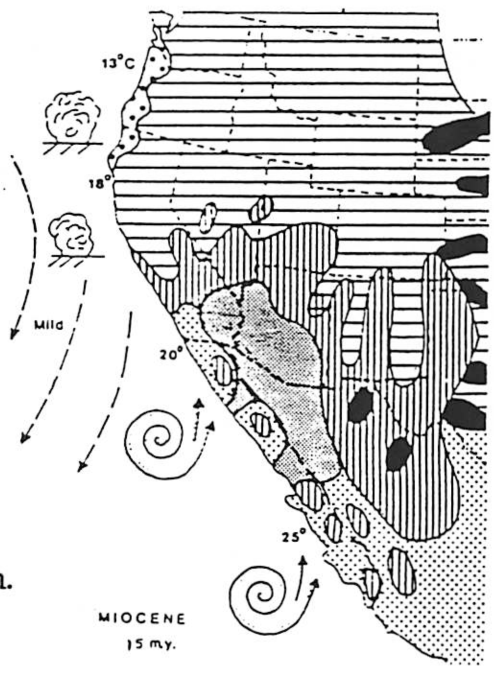

Stutfens

MIOCENE - PLIOCENE (12 - 5 my) Baja splits; endemic genera evolve; Sierra Nevada rises and results in final drying of Great Basin and Mohave deserts.

PLIOCENE - PLEISTOCENE - HOLOCENE Thorn forest and oak woodland expand during glacial periods; desertscrub expands during interglacials. Creosote migrates from South America through Chihuahuan, Sonoran and Mohave deserts.

18,000 b.p.

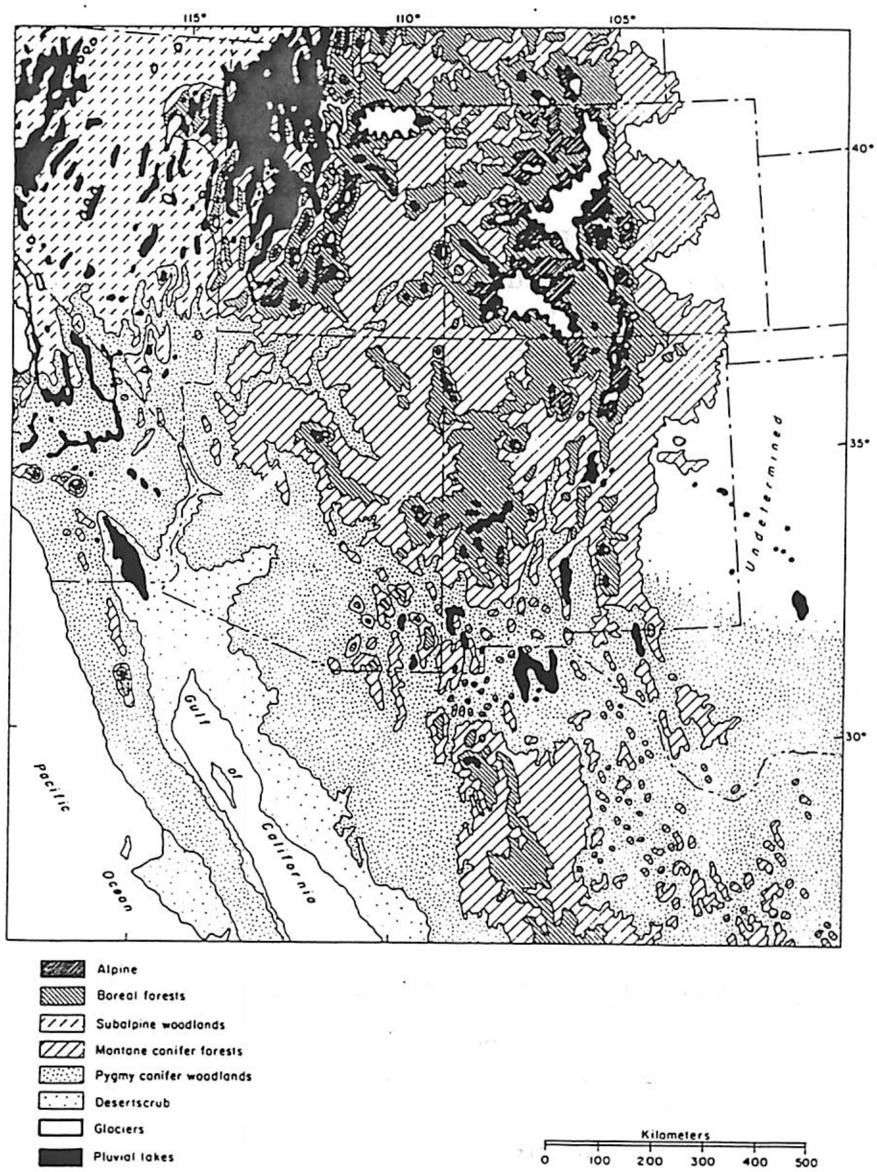

Fig. 21.1. Late Wisconsin vegetation of rocky terrain in the arid interior of western North America (see explanation in text).

Betancourt, Martin, Van Devender, 1990
Packrat Middens